5-1981

Cyclic Voltametry Studies of Various Ylide Metallocenes

Mark Mojesky
Western Kentucky University

CYCLIC VOLTAMMETRY STUDIES OF VARIOUS YLIDE METALLOCENES

A Thesis

Presented to

the Faculty of the Department of Chemistry

Western Kentucky University

Bowling Green, Kentucky

In Partial Fulfillment

of the Requirements for the Degree

Master of Science

by

Mark Twining Mojesky

May 1981

AUTHORIZATION FOR USE OF THESIS

Permission is hereby

☑ granted to the Western Kentucky University Library to make, or allow to be made photocopies, microfilm or other copies of this thesis for appropriate research or scholarly purposes.

☐ reserved to the author for the making of any copies of this thesis except for brief sections for research or scholarly purposes.

Signed Mark T. Mojesky

Date 4-7-81

Please place an "X" in the appropriate box.

This form will be filed with the original of the thesis and will control future use of the thesis.

CYCLIC VOLTAMMETRY STUDIES OF

VARIOUS YLIDE METALLOCENES

Recommended 3-30-81
(Date)

Norman L. Holy / Al Bouchu
Director of Thesis

John T. Riley

Curtis C. Wilkins

David R. Hartman

Approved 4-10-81
(Date)

Elmer Gray
Dean of the Graduate College

ACKNOWLEDGEMENTS

I would like to express my deepest gratitude and appreciation to the following persons:

Dr. Norman Holy for his guidance through this project, his inspiration and concern, and for his unselfish assistance throughout the duration of my graduate study.

Dr. John Riley, who stepped in to replace my director, Dr. Holy who had gone to Germany on sabbatical, for his helpful suggestions and critical reading that helped write this thesis.

Dr. Curtis Wilkins for his assistance and guidance throughout my graduate study.

Dr. David Hartman who stepped in to fill my thesis committee (short one member because of the absence of Dr. Holy).

Dr. Frank Toman for his inspiration and helpfulness throughout my academic years at W.K.U.

Jean Almand and Judy King for their helpfulness and unselfishness which will always be remembered.

BIOGRAPHICAL SKETCH

Mark Twining Mojesky (1956-)

The author was born [redacted] in Hartford, Connecticut. In 1974 he graduated from South Catholic High School and enrolled in Catawba College in Salisbury, North Carolina. In 1978 he received a B.S. degree in chemistry with a minor in history. In August, 1978, he enrolled in the Graduate College of Western Kentucky University and has been pursuing a Master of Science degree in Chemistry since that time.

TABLE OF CONTENTS

LIST OF FIGURES

List of Figures (continued)

List of Figures (continued)

List of Figures (continued)

LIST OF TABLES

CYCLIC VOLTAMMETRY STUDIES OF VARIOUS YLIDE METALLOCENES

Mark Twining Mojesky 98 Pages

Directed by: Norman L. Holy, John T. Riley, David R. Hartman and Curtis C. Wilkins

Department of Chemistry Western Kentucky University

The redox potentials of $[Fe(CpSMe_2)_2]^{2+}$ ($CpSMe_2$= dimethysulfoniumcyclopentadienylide), $[Ni(CpSMe_2)_2]^{2+}$, $[Co(CpSMe_2)_2]^{2+}$, $[Mn(CpSMe_2)_2]^{2+}$, $(CpPPh_3)HgBr_2$ ($CpPPh_3$= triphenylphosphoniumcyclopentadienylide), $(CpPPh_3)HgCl_2$, and MoPC (PC = phthalocyanine) were examined using cyclic voltammetry (CV). The experimentation was carried out in a temperature controlled environment. With the exception of the mercury and molybdenum complexes, the solvent system consisted of 15 milliliter mixture of acetonitrile and water. Due to the solubility problems of the mercury bromide complex, dimethylformamide (DMF) was used as the solvent. Pure acetonitirile was used for the mercury chloride and molybdenum complexes.

The emphasis of this research was directed towards the iron complex. Its complimentary pure metallocene $FeCp_2$(Cp = cyclopentadiene) is well characterized, thereby permitting a comparison of the two complexes. The iron sulfonium ylide complex was found to have lower redox potentials. This supports the anticipated effect of the added dimethylsulfonium (SMe_2) group.

I. INTRODUCTION

Metallocenes are placed in the general class of π-bonded organometallic compounds. Ferrocene, bis(cyclopentadienyl)-iron(II) is the metallocene that has been the most extensively studied. The structure of metallocenes generally consists of two parallel cyclopentadiene rings with the metal atom sandwiched between them. This structure is pictured with two possible conformations in Figure 1.

eclipsed (a) staggered (b)

Figure 1. Two conformations of metallocenes

Ferrocene ($FeCp_2$) was the first metallocene to be synthesized. It was discovered by Kealy and Pauson[1] through an unsuccessful attempt to prepare dihydrofulvalene ($C_5H_5{=}C_5H_5$). Their unexpected product resulted from the reaction between cyclopentadienylmagnesium and ferric chloride in diethyl ether. Ferrocene was also prepared by Miller, Tebboth, and Tremaine[2] approximately the same time by passing cyclopentadiene vapor over a special iron-molybdenum catalyst. Wilkinson,

Rosenblum, Whiting, and Woodward[3] suggested the pentagonal structure [Figure 1(b)] which was later confirmed by X-ray crystallography.[4,5] The known metallocenes and some of their related compounds are listed in Table 1.

In 1953, Wilkinson, Pauson, and Cotton[6] began an electrochemical study of the bis(cyclopentadienyl) compounds of nickel and cobalt. They reported the oxidation of $Ni(II)Cp_2$ to $Ni(III)Cp_2^+$ in a 90% ethanolic electrolytic medium at -0.08V versus the SCE. Disruption of the molecule resulted when further oxidation to the dipositive ion was attempted.[7]

Similar results were observed by Wilson, Warren and Hawthorne[7] in their study of Ni(IV). When the medium (acetonitrile) was cooled to -40°C, two reversible processes appeared as shown by Figure 2. The reduction peak at +0.77V shows the existence of the d^6 nickel(IV) ion. It was noted that the species decomposed rapidly at temperatures above 0°C. A summation of their studies is given in Table 2.[7]

The electroreduction of cobaltocene was reported by Geiger in 1974.[8] Through the use of polarographic and cyclic voltammetric techniques, the cobaltocene anion, $CoCp_2^-$ was generated. This species was the third member of the reduction process consisting of $CoCp_2^+$, $CoCp_2$, and $CoCp_2^-$. Following is a depiction of the reduction process:

$$CoCp_2^+ + e^- \longrightarrow CoCp_2 \qquad (1)$$

$$CoCp_2 + e^- \longrightarrow CoCp_2^- \qquad (2)$$

$$CoCp_2^- + e^- \longrightarrow Z \qquad (3)$$

Where Z was some unknown product. The reduction peaks corresponding to systems (1) and (2) were recorded at -0.94V

Table 1

Some Metallocenes and Related Compounds

Group	III	IV	V	VI	VII	VIII	VIII	VIII	Ib
3d Series		$(TiCp_2)_n$ $TiCp_2Cl_2$	VCp_2 VCp_2Cl VCp_2Cl_2	$CrCp_2$ $[CrCp_2]^+I^-$	$MnCp_2$ $Mn[Cp(CH_3)_5]_2$	$FeCp_2$	$CoCp_2$	$NiCp_2$	
4d Series		$(ZnCp_2)_n$		$MoCp_2H_2$	$TcCp_2H$	$RuCp_2$	$RhCp_2$ Rh_2Cp_4 Rh_3Cp_4H	Pd_2Cp_4	
5d Series	Various Lanthanide & Actinide Compounds $MCp_{3,4}$		$TaCp_2H_3$	WCp_2H_2	$ReCp_2H$	$OsCp_2$	$IrCp_2$ Ir_2Cp_4	Pt_2Cp_4	$(AuCp)_n$

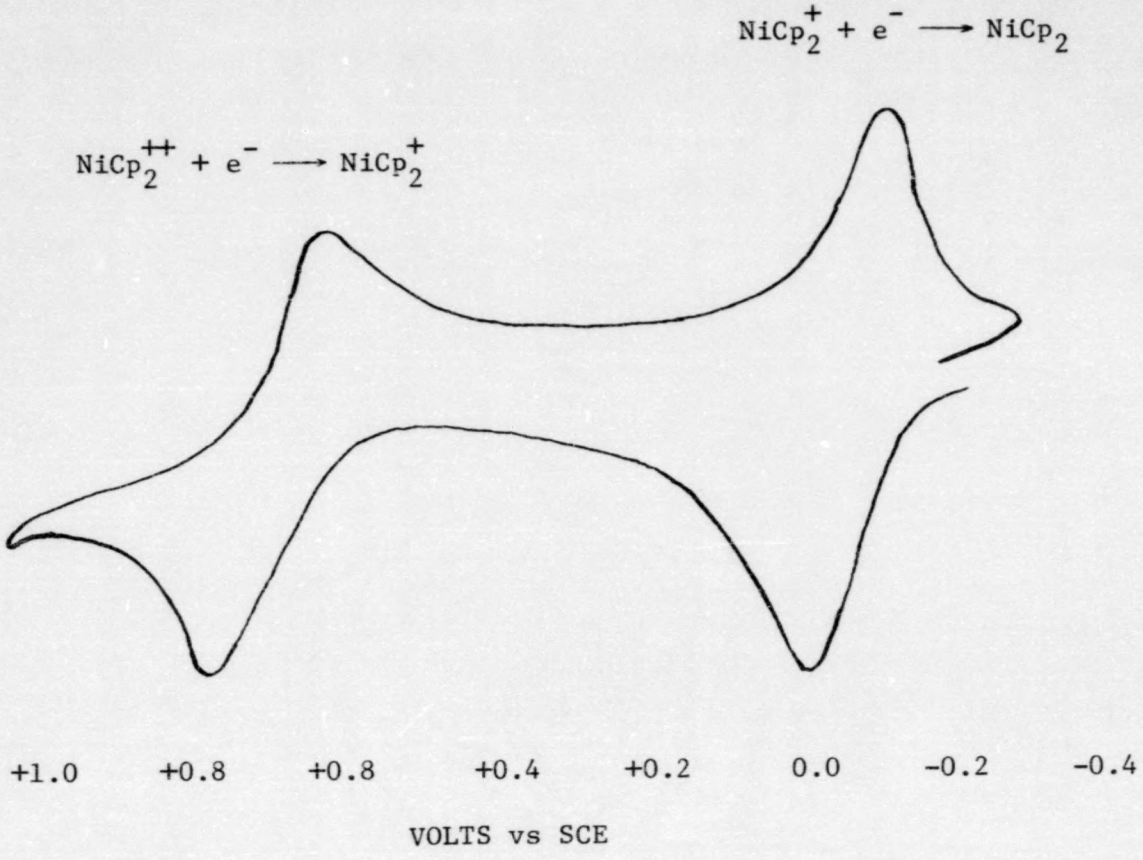

Figure 2. Cyclic voltammogram of the $Ni(\pi\text{-}C_5H_6)_2$ in acetonitrile solution at -40°C

Table 2

Reduction Peak Potentials of the
π-Cyclopentadienyl π-(3)-1,2-Dicarbollynickel Complexes

Compound	$M(IV)+e^- \rightarrow M(III)$	$M(III)+e^- \rightarrow M(II)$
$Ni(C_5H_5)_2$	Dication $\xrightarrow{+0.77}$ cation	Cation $\xrightarrow{-0.09}$ neutral
$(C_5H_5)Ni(B_9C_2H_{11})$	Cation $\xrightarrow{+0.46}$ neutral	Neutral $\xrightarrow{-0.52}$ anion
$Ni(B_9C_2H_{11})_2$	Neutral $\xrightarrow{+0.18}$ anion	Anion $\xrightarrow{-0.56}$ dianion

and -1.88V (versus the SCE) respectively. The appearance of the peaks indicated that processes (1) and (2) are highly reversible.

Once the redox systems of the more stable metallocenes had been examined, studies shifted to those that were more air-sensitive. The first to be studied was bis(cyclopentadienyl)chromium(II), $CrCp_2$.[9,10] The compound proved to be stable under the experimental conditions used. A dc polarogram of the metallocene in acetonitrile showed an oxidation wave of -0.67V which corresponds to a one-electron oxidation to $CrCp_2^+$. The proposed reversibility was confirmed by cyclic voltammetry (Figure 3).

Geiger continued his work which led to studies of vanadocene, vanadocene chloride, nickelocene, and chromocene.[11] High vacuum and low temperature techniques were employed in conjunction with electrochemistry to characterize VCp_2, $CrCp_2$, and $NiCp_2$. The results can be seen in Table 3. Vanadocene, the most electron deficient metallocene, was observed to be easily oxidized in dual one-electron steps. The oxidation of vanadocene [V(II) $\longrightarrow$ V(III) + e^-] proved to be reversible and not to involve any structural changes.

The data obtained on chromocene showed it was oxidized in dual one-electron steps. The suggested process is shown below.

$$CrCp_2^+ \underset{\longleftarrow}{\xrightarrow{e^-}} CrCp_2 \underset{\longleftarrow}{\xrightarrow{e^-}} CrCp_2^-$$

The system was found to be reversible when carried out in tetrahydrofuran.

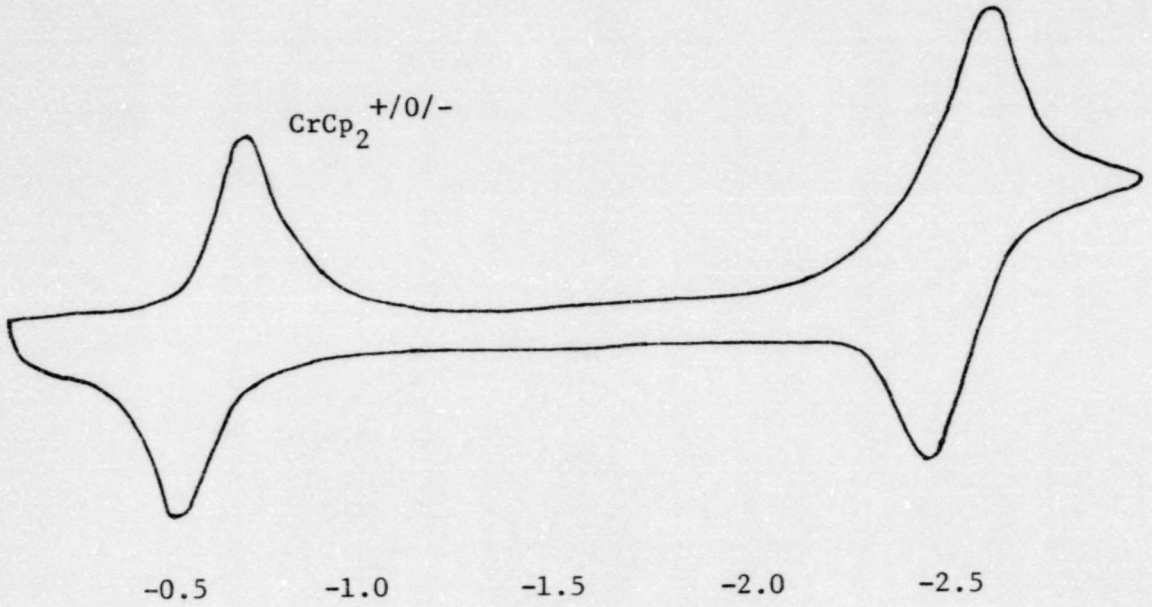

Figure 3. Cyclic voltammogram of $CrCp_2$ in THF at a platinum electrode at a scan rate of 100 mV/S, showing the reversible oxidation to $CrCp_2^+$ and reduction to $CrCp_2$.[10]

Table 3

Polarographic $E_{1/2}$ Values for Metal π Complexes

Metallocenes

Compound	Solvent	2+ ⇌ 1+	1+ ⇌ 0	0 ⇌ 1-
VCp_2	THF	+0.59	-0.55	-2.30
$CrCp_2$	CH_3CN		-0.67	-2.30
$FeCp_2$	CH_3CN		+0.31	
$CoCp_2$	CH_3CN		-0.94	-1.88
$NiCp_2$	CH_3CN	+0.74	-0.09	-1.66

Nickelocene was the easiest of the metallocenes to be reduced (smallest reduction potential) despite its being the most electron-rich metallocene known. The cyclic voltammogram (CV) of $NiCp_2$ can be seen in Figure 4. Gubin et al.[12] has proposed that the reduction of nickelocene occurs in the following manner:

$$NiCp_2 + 2e^- + 2H^+ \longrightarrow$$

The results obtained by Geiger and Holloway show the reduction is very complex and the nickelocene anion is only stable at low temperatures. Their work showed that at -58°C in DMF, the anion was indeed stable, but the electron transfer process was very slow for the reduction.

In summary, the redox studies show that $NiCp_2$ is the only metallocene that exists as four distinct species ($NiCp_2^{2+}$/+/0/-1). Vanadocene has dual, one-electron transfer steps as does $CrCp_2$ and $CoCp_2$.

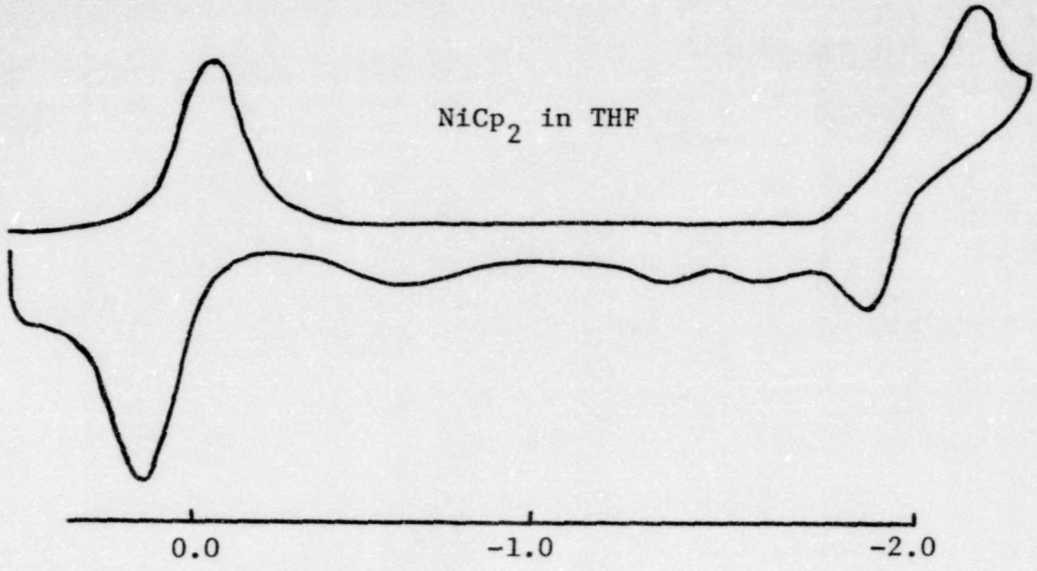

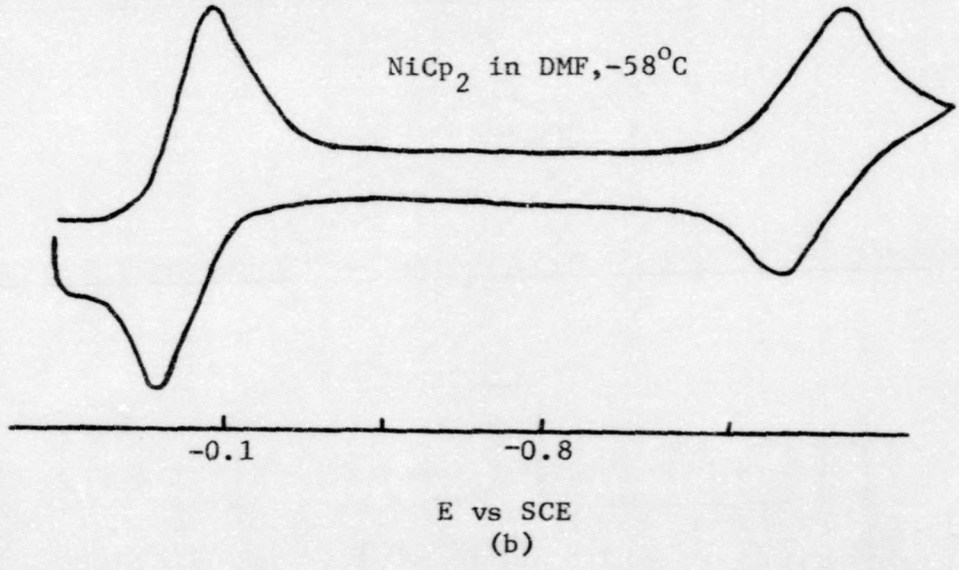

Figure 4. Cyclic voltammograms of $NiCp_2$ in THF (a) and DMF (b)

II. THEORETICAL CONSIDERATION OF CYCLIC VOLTAMMETRY

A. General Theory

Cyclic voltammetry is considered to be a very effective technique that enables one to observe peaks due to the oxidation and/or reduction of a species by scanning the potential of a working electrode in the anodic or cathodic direction. The electrode system used is governed by the nature of the medium as well as the substrate being studied. The conventional instrumentation used in cyclic voltammetry is quite simple. It consists of a three electrode system (working, reference, and auxiliary), a triangular wave generator, and a X-Y recorder which records the voltammograms. Some of the more common types of working electrodes are the carbon paste electrode, hanging mercury drop electrode, platinum wire electrode, and planar platinum disk electrode.

The technique involves a repetitive wave which is generated in an isosceles triangular form (Figure 5A). Sevik[13] was the first scientist to employ such a technique. The potential at the working electrode is obtained by sweeping back and forth between two specific potentials (switching potentials). If the scan is carried out from one designated value to the other and back again, the cycle is complete, thus termed cyclic voltammetry. This cycle can be produced once, or several times, depending on the nature of the experiment (the dotted isosceles triangle in Figure 5A

represents a second cycle). A potential scan from +0.5V to -0.5V is shown in Figure 5B. The scanning window in Figure 5C uses the entire range of +1.0V to -1.0V. The wave generator should be capable of producing sweep rates ranging from about 0.02V/sec. to 1000V/sec. Values of 10-100 V/min. usually produce the most reliable results.[14]

Once the location of the redox couple of interest is determined, a cyclic voltammogram can be obtained. During the potential scan, the current at the working electrode in an unstirred solution is measured. A typical voltammogram of Fe^{2+} in 1 M H_2SO_4 obtained with a carbon paste electrode is shown in Figure 6. At point a, the scan is initiated in the anodic direction with Fe^{2+} as the species in solution. Depletion of Fe^{2+} and the increase in concentration of Fe^{3+} (oxidation) is accompanied by an increase in current (b). The concentration of Fe^{2+} approaches zero at the electrode surface at point c and as the peak potential (E_{pa}) is reached. At this point the system becomes diffusion controlled, and the current drops to near zero as the scan is continued in the positive direction. Once the switching potential is reached, the potential scan now moves cathodically. The current remains near zero until the potential for the reduction of Fe^{3+} to Fe^{2+} is reached at which the current (i_{pc}) begins to increase. The cathodic or reduction potential (E_{pc}) is reached at point g. Thus, in this system Fe^{2+} is initially oxidized to Fe^{3+} and subsequently reduced to the original species.

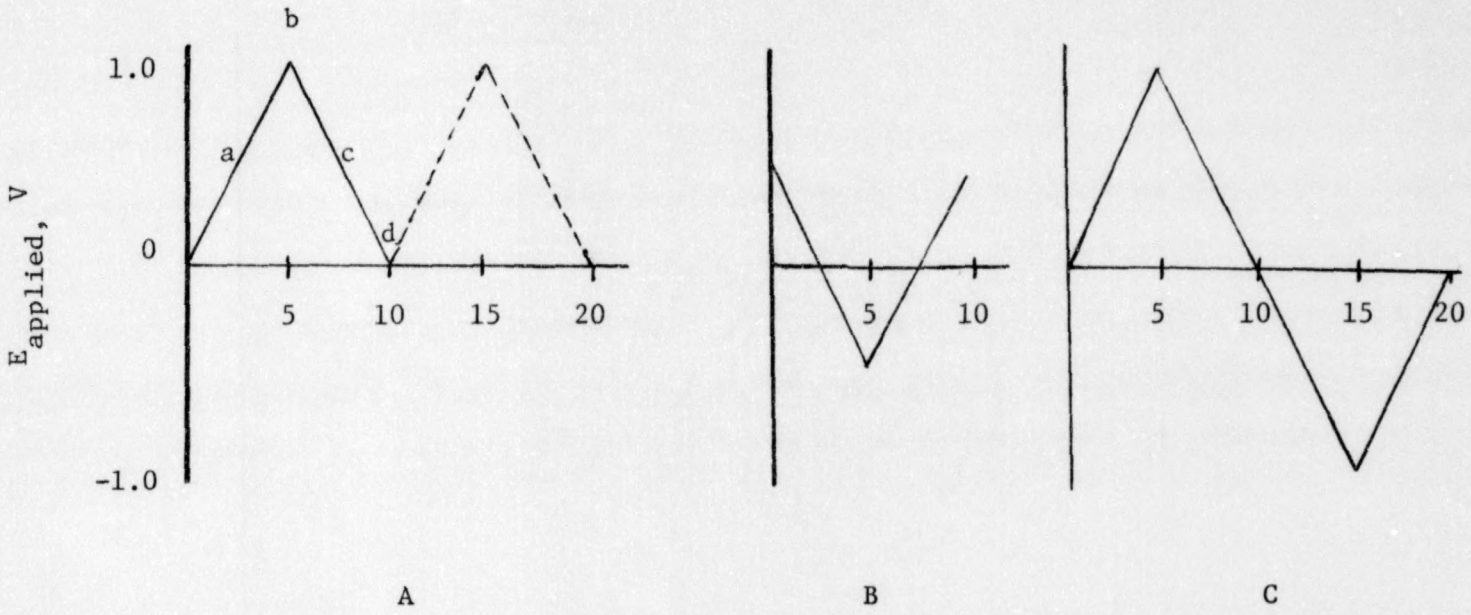

Figure 5. Applied potential (E)-time profiles for cyclic voltammetry.

The labeled portions of Figure 5A can be interpreted in the following way:

a. positive potential scan from 0V to 1.0V
b. switching potential
c. negative potential scan from +1.0 to 0V
d. termination of the first cycle

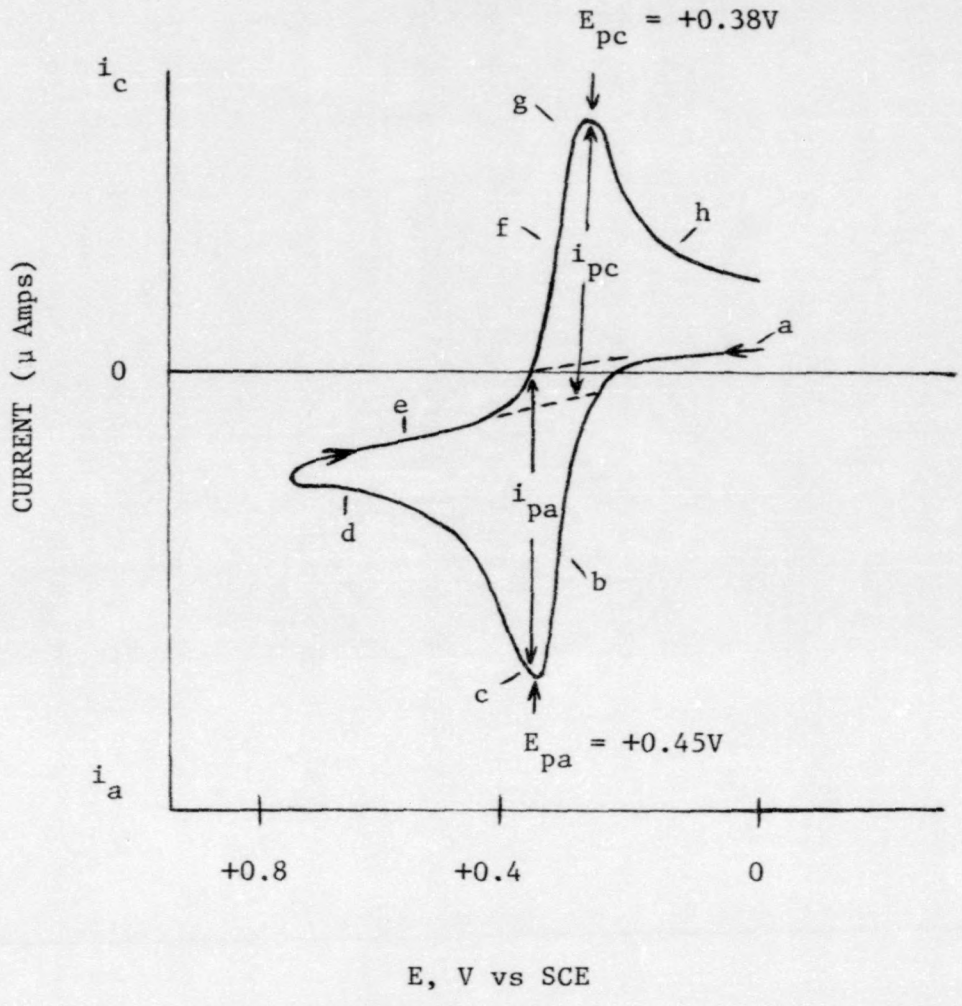

Figure 6. Cyclic voltammogram of Fe^{2+} in 1 M H_2SO_4.[14]

The waves produced from cyclic voltammetry represent two general processes: reversible (Figure 7A) and irreversible (Figure 7C). The wave in Figure 7B represents a quasi-reversible process which is somewhere between the two mentioned above. The difference in the rate at which the electron(s) is(are) transferred is the primary cause of the differences in the processes and consequently the shapes of the waves. A reversible process voltammogram results from a fast electron transfer process whereas an irreversible process voltammogram results from a slow electron transfer process. As seen in Figure 7, the peaks of an irreversible process wave are much broader, flatter, and the peak separation greater when compared to reversible process wave.

The detection of a reversible system depends on several criteria. One very important numerical consideration is the difference between the cathodic and anodic peak potentials as illustrated in the following relation:

$$E_{pa} - E_{pc} \approx 2(0.029/n) = \frac{0.059}{n} \text{ V} \qquad \text{(II-1)}$$

where n = number of e^-'s transferred. If, for example, a redox couple was shown to have a one-electron reversible transfer process, the peak potential difference should be approximately 0.059V. It is important to realize that equation II-1 applies only to a reversible system and holds for single-sweep voltammograms of individual solutions, one for oxidation and one for reduction. The conditions for cyclic voltammetry are slightly different. In the previous discussion it was stated that the concentration of Fe^{2+} was effectively zero

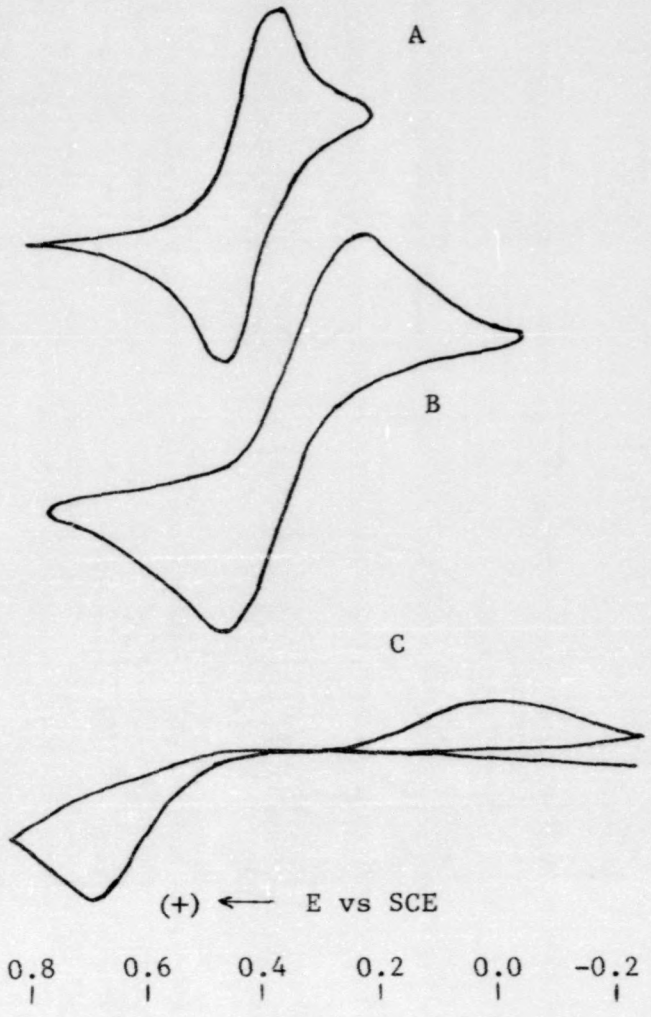

Figure 7. Cyclic voltammograms as a function of charge-transfer rate.

A) reversible,
B) quasi reversible
C) irreversible

at the electrode surface when the peak potential, E_{pa}, is reached. This is not entirely true. The concentration of Fe^{2+} becomes zero only after the peak potential has been passed. Therefore, the initial condition for the anodic reversal is not the same as for the starting cathodic sweep. A small anodic shift of the oxidation wave results, making the peak separation slightly greater than the ideal value predicted by equation II-1.[15]

The peak current (i_p) is an important concept in understanding voltammetry. The peak current for a reversible system at 25°C is defined by the Randles-Sevik equation.

$$i_p = 269\ n^{3/2} A D^{1/2} C^b V^{1/2} \qquad \text{(II-2)}$$

where i_p is the peak current; n is the number of electrons transferred; A is the electrode area (cm^2); D is the diffusion coefficient of the species being oxidized or reduced (cm^2/sec); C^b is the concentration of the species in bulk solution (mole/ℓ); and V is the scan rate (V/sec).

According to equation (II-2), the peak current is directly proportional to the square root of the scan rate. Because of this proportionality, a straight line is obtained when the peak current (i_p) is plotted against the square root of the scan rate. If, for example, the scan rate is increased in intervals and all other parameters held constant, a straight line through the origin should result with a reversible couple. When faster scan rates are employed, less time is available for consequent depletion of the original species. Thus, the result is an increase in peak current. It should be noted

that for a reversible couple the peak potential will remain constant if and when the scan rate is varied.

For an irreversible couple the peak current equation is

$$i_p = 3.01 \times 10^5 \, n(\alpha N_a)^{1/2} A D^{1/2} C^b v^{1/2} \qquad \text{(II-3)}$$

and obviously much more complicated than that for a reversible system. The new terms α and N_a are the transfer coefficient and the number of electrons in the rate-determining step of the electrode process respectively. For a reversible system the concentration at the electrode surface is determined by the Nernst equation and is therefore independent of the scan rate. This is not true for an irreversible couple. The peak potential is given by

$$E_p = E^o + \frac{RT}{\alpha nF} \; -0.78 + \ln \frac{k_1}{D_o^{1/2}} - (1/2) \ln \frac{\alpha nF}{RT} v \qquad \text{(II-4)}$$

where k_1 is related to the rate constant. The remaining terms not previously defined, F, R, and T, have their usual connotation.

The peak current of a voltammogram has to be carefully measured if it is to be used as a criterion for analyzing systems. It is best accomplished by directly measuring the X-Y recording. A suitable method was developed by Hawley and Adams.[16,17] Figure 8 represents an illustration of the procedure used to obtain correct and accurate values for a sweep begun in the anodic direction. Often parts of the curve have to be extrapolated (pts. C,D) in order to obtain a steady baseline, a necessity in obtaining correct i_p values. When the system is as simple as the one depicted in Figure 8,

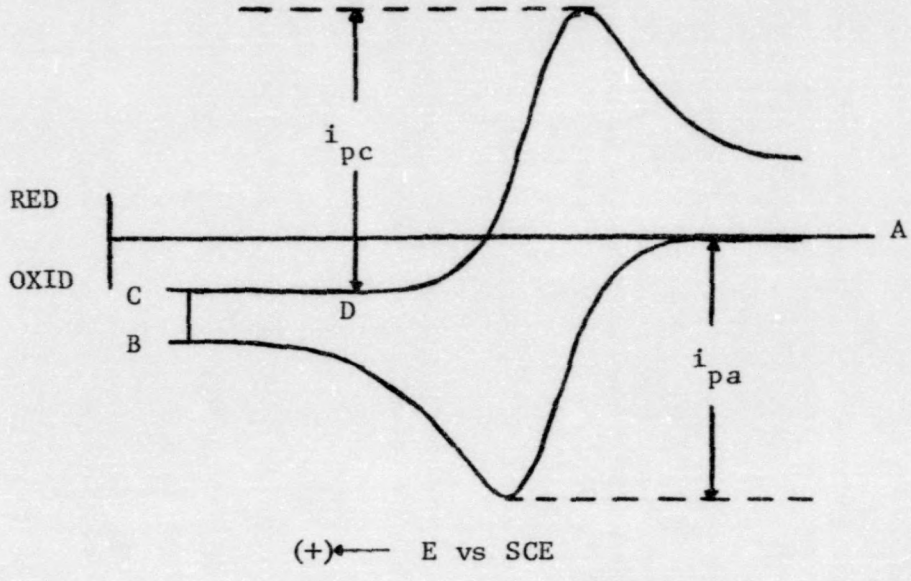

Figure 8. Potential hold method of measuring true reverse peak current.

an accurate measurement can be obtained. In the case of successive reactions the system becomes much more complex as does the extrapolation. One way to solve this problem is to terminate the scan at some point before the second wave appears and after the first has past. Figure 9 represents this procedure where the scan is terminated at A (the dotted line represents a second wave). Thus, the first peak can be analyzed. If the second successive reaction needs to be interpreted, the scan can be continued and stopped just as the previous cycle was. The potential will remain in position wherever the scan is stopped. A procedure for analyzing consecutive reactions for the peak current was developed and used by Schwartz and Shain.[18] A second method developed by Nicholson[19] employs a procedure that measures the current directly from a complete cyclic voltammogram and does not involve holding times. Although these methods seem adequate, one should realize that accurate peak current values can only be obtained from ideal systems (Figure 8). As the redox couples become more complex, i_p values are less accurately obtained.

Chemical reactions coupled to the electrode process influence the ratio of the peak current heights (i_a/i_c). A method developed by Nicholson and Shain[20] uses this ratio as a method to characterize the system. The following cases are examples:

Case A: Reversible electron transfer: $O + ne^- \rightleftharpoons R$

The voltammograms observed show anodic and cathodic peaks identical in shape and height. They are also

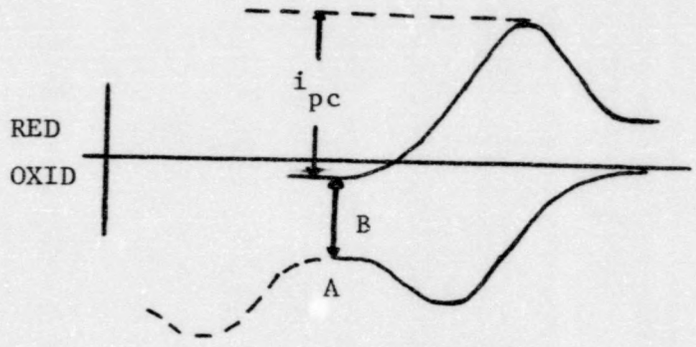

Figure 9. Potential hold method for cases of successive reactions.

independent of the scan rate. The ratio of the peak current heights are on a 1:1 basis. This diagnosis demonstrates the absence or unimportance of any subsequent chemical reaction.

Case B: Reversible chemical reaction preceeding a reversible electron transfer: $Z \underset{k_b}{\overset{k_f}{\rightleftharpoons}} O$, $O + ne^- \rightleftharpoons R$

The anodic wave lies virtually unaffected by the preceeding chemical reaction when compared to the cathodic region. The cathodic region becomes flat and broad. As the sweep rate is increased, the anodic peak current height increases as well. Therefore, the ratio of the peak current height (i_a/i_c) will increase as the scan rate increases.

Case C: Electron transfer followed by a reversible chemical couple: $O + ne^- \rightleftharpoons R$, $R \underset{k_b}{\overset{k_f}{\rightleftharpoons}} Z$ where Z is some product.

A fairly large number of organic reactions fit this type of mechanism. The cathodic wave is now very sensitive to the scan rate. The peak current height decreases at a much faster rate than the anodic portion when the sweep rate is increased. The final result obtained is a smaller i_a/i_c ratio as the scan rate increases.

Case D: Electron transfer preceeding an irreversible chemical reaction: $O + ne^- \rightleftharpoons R$, $R \xrightarrow{k_f} Z$

The cathodic wave is greatly affected by the scan rate. Although the peak current (i_{pc}) remains constant, the peak potential (E_{pc}) does not. On the anodic portion of the voltammogram, the E_{pa} remains constant and the i_{pa} changes. At slow scan rates the (i_a/i_c) ratio is less than one as a

result of small i_a values. The ratio becomes closer to unity as the sweep rate is increased.

Case E: Catalytic reaction with reversible electron transfer:

$$O + ne^- \rightleftharpoons R, \quad R + Z \xrightarrow{k'_f} O$$

This case, being similar to case A, has cathodic and anodic waves similar in shape and independent of the scan rate. The ratio of the peak current heights is again unity. Quantitatively an increase in the current would be the effect of the chemical reaction on the cathodic portion of the system.

A graphical summary of the five cases is shown in Figure 10. By using this method of analysis, cyclic voltammetry becomes a powerful tool for studying mechanisms of redox reactions.

Separation of the cathodic and anodic peak potentials were used by R. S. Nicholson[21] to measure rate constants for electron transfer. The presence of homogeneous reactions in the reaction mechanism is easily detected and the interpretation simple. Therefore, a direct method for electrode reversibility is available assuming the following mechanism:

$$O + ne^- \underset{k_b}{\overset{k_f}{\rightleftharpoons}} R$$

Nicholson related the absolute rate theory to the electrode process and a numerical solution of an integral equation provided a correlation between the ΔE_p's with the function ψ

$$\psi = \nu^{\alpha} \frac{k_s}{[\pi D_O (nF/RT)V]^{1/2}} \qquad \text{(II-5)}$$

where V is the scan rate (V/sec), ν is the square root of the ratio of the diffusion coefficients D_O and D_R, α is the

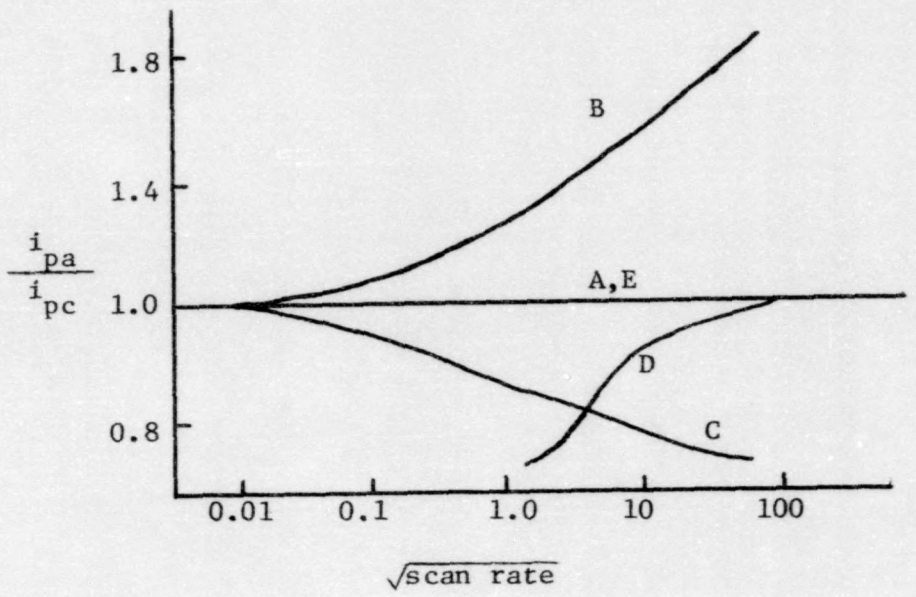

Figure 10. Variation in the ratio of anodic to cathodic peak currents as a function of the square root of the scan rate for several electrode processes with a reversible electron transfer.[20]

transfer coefficient and k_s is the standard rate constant at $E = E^o$. The remaining terms have their usual meaning. For many practical situations ν^α is unity since the difference in the diffusion coefficients are so small. Equation II-5 can therefore be simplified to

$$\psi \simeq 28.8 \frac{k_s}{v^{1/2}} \qquad \text{(II-6)}$$

by using the approximation $\nu^\alpha = 1 \times 10^{-5}$ cm^2/sec, and F/RT = 38.9 V^{-1}. A relation between ψ and ΔE_p was developed through a working curve shown in Figure 11. The data used to construct the curve is listed in Table 4. From this correlation one can simplify equation II-6 even further by using the approximate values of ψ. Table 4 and Figure 11 show ψ to be optimum at 0.5 for most measuring purposes. Therefore,

$$0.5 = 28.8 \frac{k_s}{v^{1/2}} \qquad \text{(II-7)}$$

It can be concluded that for very fast electron transfer systems the required scan rate needs to be quite fast also.

It is sometimes possible to tune the system until it becomes reversible.[22] One might apply this technique if the study of rate constants were the prime objective. Nicholson[21] explains the process well. An example of such a process can be seen in Figure 12. When the optimum scan rate is located (to obtain a reversible couple) a distinct difference in the E_p can be observed.

B. Qualitative Applications of Organic Substrates

Cyclic voltammetry can provide valuable information about electrode processes that occur during the oxidation

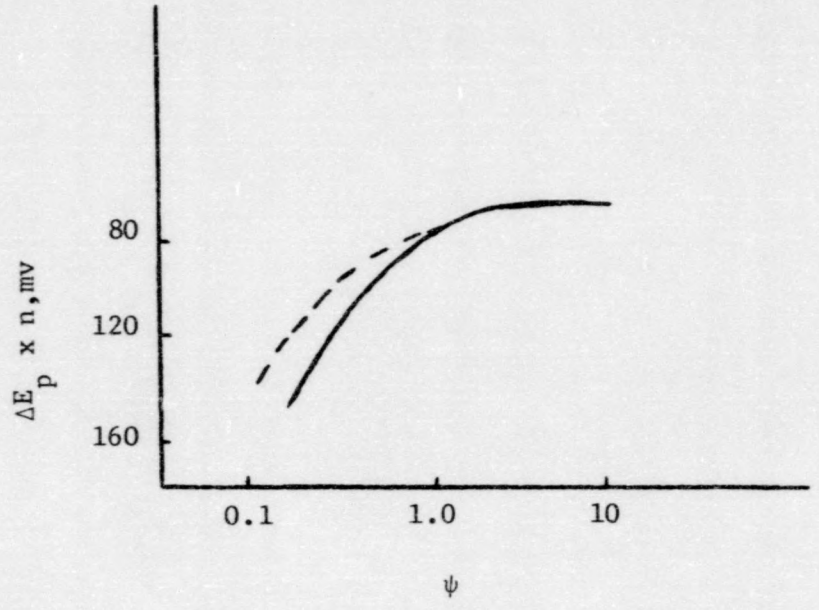

Figure 11. Working curve showing variation of peak potential separation (ΔE_p) with ψ.[21]

Table 4

Variation of Peak Potential Separations with Kinetic Parameters for Cyclic Voltammetry.[21]

ψ [a]	$\Delta E_p \times n$ [b] MV
20	61
7	63
6	64
5	65
4	66
3	68
2	72
1	84
0.75	92
0.5	105
0.35	121
0.25	141
0.1	212

[a] $\psi = \nu^{\alpha} Ks/[\pi D_o(nF/RT)V]^{\frac{1}{2}}$

[b] For $\alpha = 0.5$

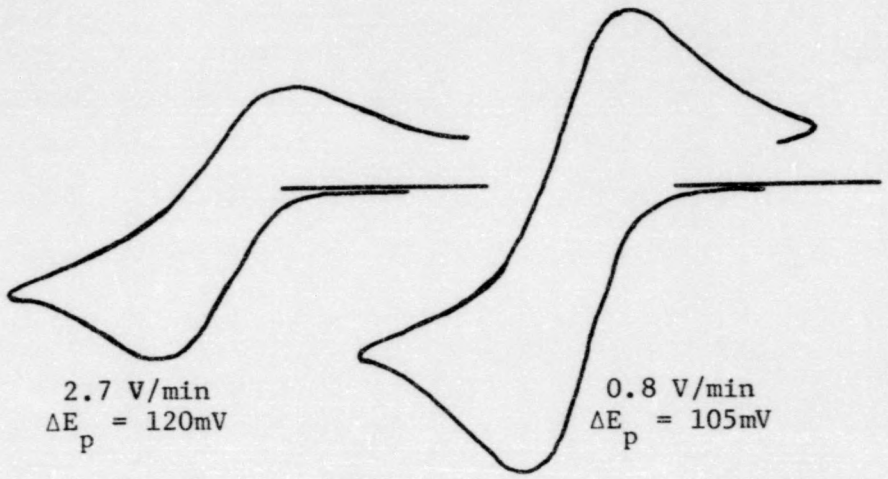

Figure 12. Measurement of charge-transfer rate via cyclic voltammetry.

or reduction of an organic compound. The usefulness of a CV in examining a reversible oxidation process is demonstrated by the oxidation of 9,10-dihydro-9,10-dimethylphenazine (DMPZ).[23]

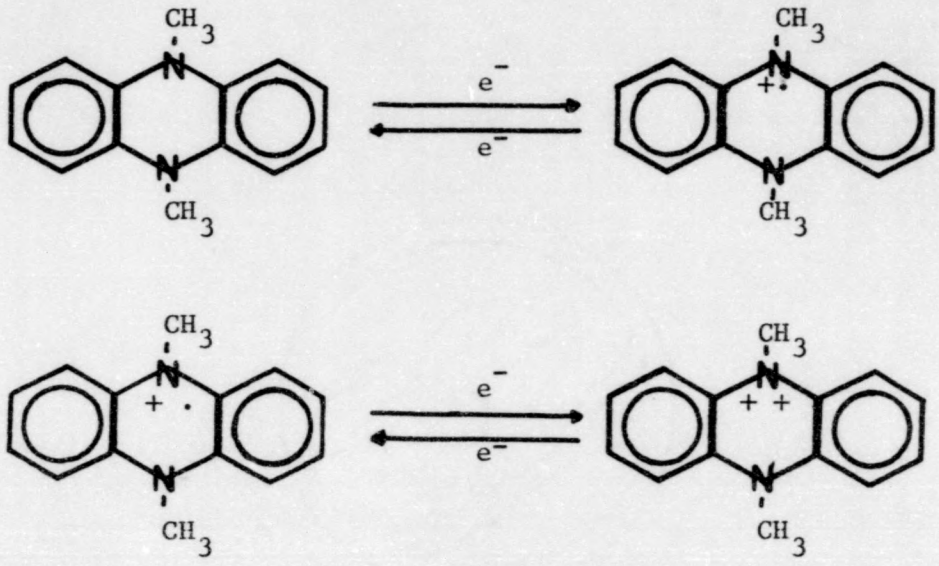

The system depicted above undergoes two successive reversible one-electron oxidation-reduction steps where the ΔE_p for the first redox couple is 58mV and for the second is 59mV. The CV redox chemistry for DMPZ has been used as a model system, to which other systems are compared.

The oxidation of 9,10-diphenylanthracene (DPA) to the cation radical has been used to demonstrate how steric effects influence the reactivity of anodically generated cation radicals with nucleophiles.[24] In the absence of a nucleophile, the oxidation of DPA fulfills the criteria for a reversible process. The CV of DPA in the presence of 3,5-lutidine gives a stoichiometric increase in the anodic peak current (Figure 13A). The redox reaction which occurs is extremely fast. The more hindered nucleophile, 2,5-lutidine,

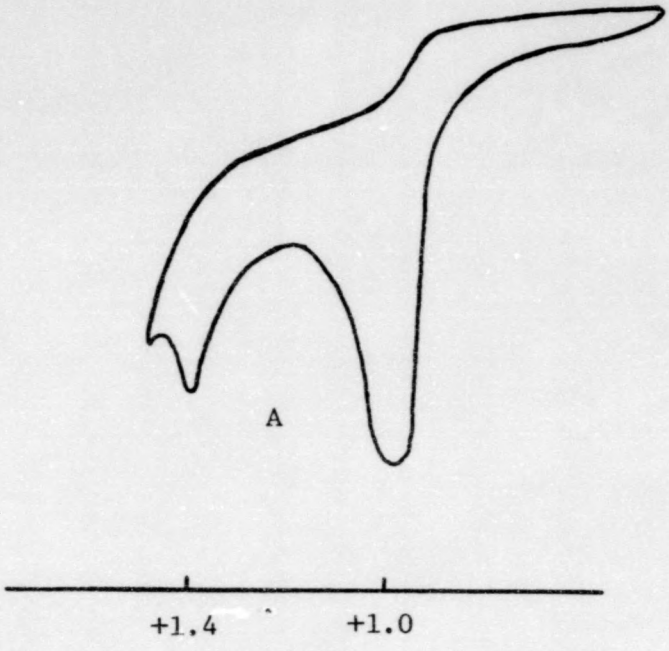

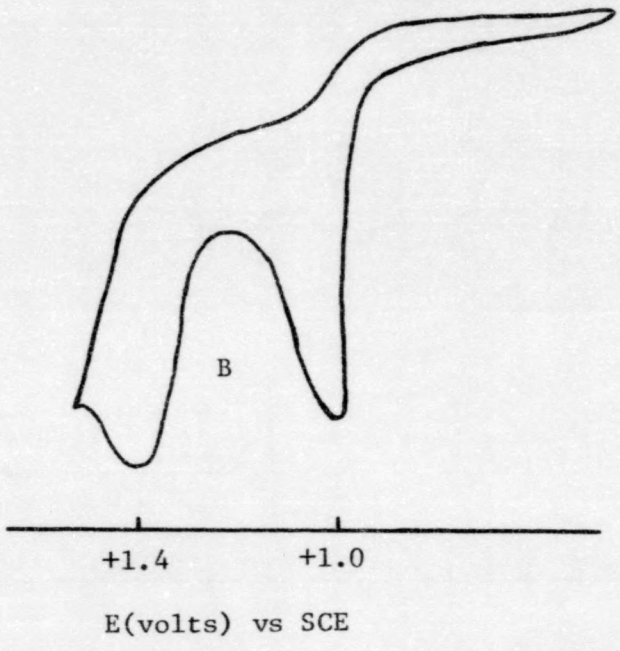

Figure 13. Voltammogram of 9,10-diphenylanthracene in the presence of 3,5-lutidine (A) and 2,5-lutidine (B).

is found to further increase the anodic peak current at 1.4 volts. The resulting CV is shown in Figure 13B.

An illustration of how cyclic voltammetry techniques can be used to study more complicated systems is shown in Figure 14. This CV represents the oxidation of 3,4-methoxy bibenzyl to 2,3,6,7-methoxy-9,10-dihydrophenanthrene. The suggested mechanism is shown below.

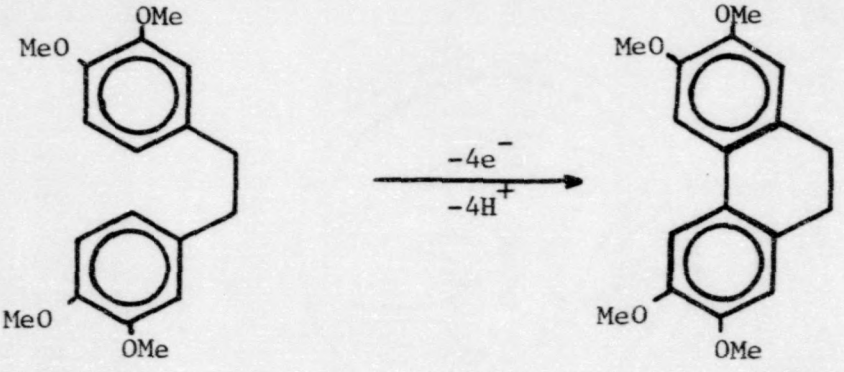

3,4-methoxy bibenzyl 2,3,6,7-methoxy-9,10-dihydrophenanthrene

The voltammogram shown in Figure 14 reveals only three peaks. On the anodic scan, the first oxidation peak (O_1) does not have a corresponding reduction wave. As the cathodic scan continues, a reduction peak (R_2) appears and is coupled with an oxidation peak (O_2) in a quasi-reversible system.

Cyclic voltammetry has become a very useful tool for estimating the stability of intermediates formed during an electrode process by varying the scan rate. For example, at slow sweeps a system may appear as a two- or multi-electron transfer process due to coupled chemical reactions and/or further oxidation of initial intermediates. It is sometimes possible to use a scan rate that is very fast compared to the speed of the coupled chemical reactions and consequently

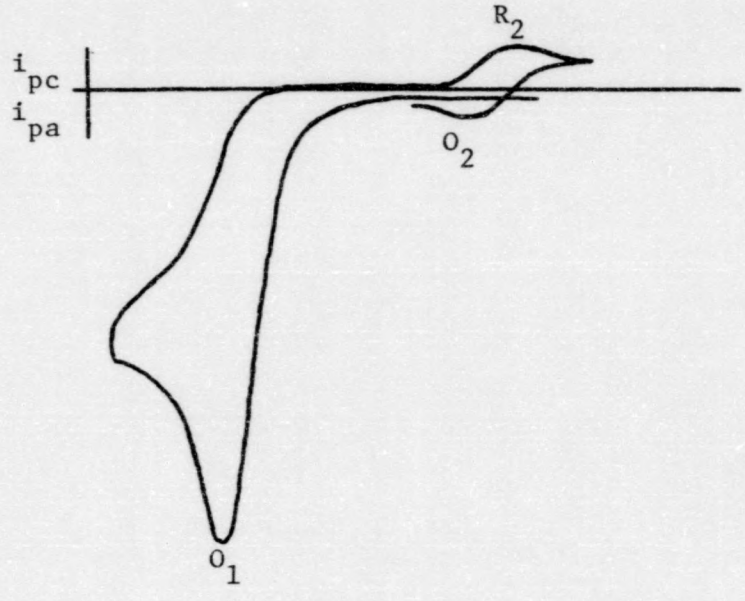

Figure 14. Cyclic voltammogram of a substituted bibenzyl undergoing oxidative cyclization to an oxidized form of a 9,10-dihydrophenanthrene.

the peaks due to the chemical reactions are not observed in the CV. This technique has been used in several instances.[25,26]

The final system to be discussed is a striking example of the effect of a follow-up chemical reaction. The oxidation of 4,4-oxydiphenol is shown in Figure 15.[27] The redox reaction took place at a carbon paste electrode in 1 M perchloric acid. The scan was initiated in the anodic direction and the first oxidation wave appears at approximately +0.4V(B). As the scan continues through a second cycle a second oxidation peak is observed (C) apparently coupled with the single reduction peak (B). This quasi-reversible couple was identified as hydroquinone-benzoquinone. It is suggested that 4,4'-oxydiphenol splits into 2 moles of benzoquinone following the initial charge transfer.

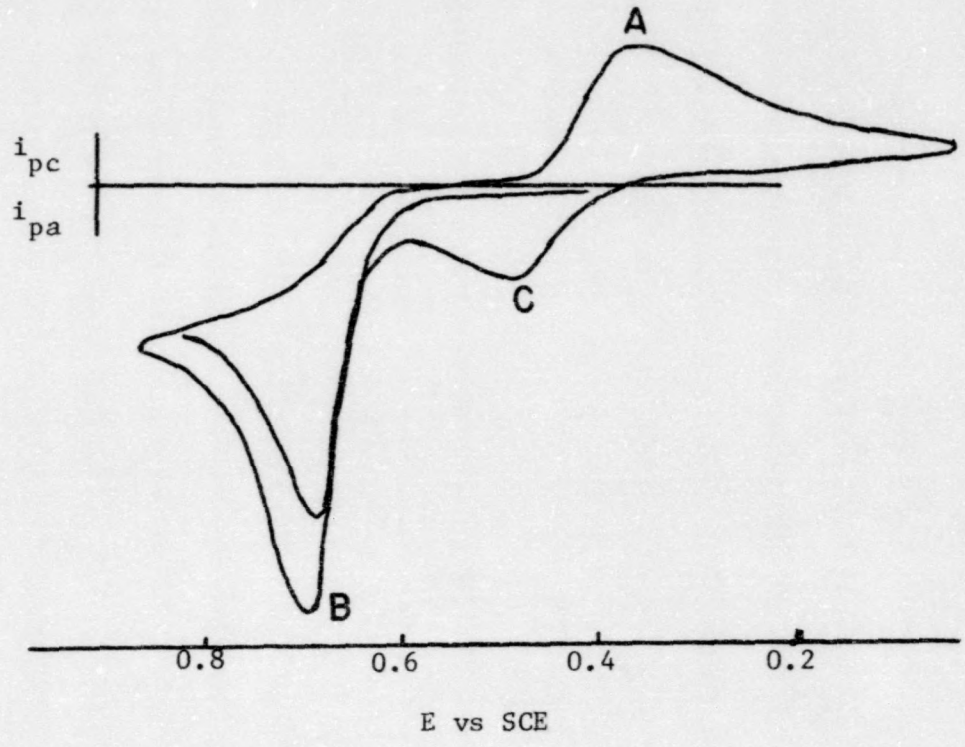

Figure 15. Cyclic voltammogram of 4,4'-oxydiphenol in 1 M perchloric acid.

III. EXPERIMENTAL

A. Apparatus

The equipment used in this research consisted of a voltammetry instrument, Model CV-1A from Bioanalytical Systems, West Lafayette, Indiana, connected to an Omnigraphic Model 2122-6-5 X-Y recorder from the Houston Instrument Company. A Haake F-Junior constant temperature circulating pump was used to control the temperature within the cell. A second circulating pump from the Gelber Company of Chicago, Illinois, was used when it was desired to lower the temperature within the cell. The electrolytic cell was a jacketed titration vessel (20 ml) from Brinkman Instruments, Inc. The electrodes used were a saturated calomel electrode (Metrohm E404), hanging mercury drop electrode (Metrohm E-410), and a carbon paste electrode (Metrohm EA267). The auxillary electrode was a platinum wire.

B. Reagents

The water used in this research was deionized, distilled, and millipore filtered. All glassware used was first boiled in a solution of $K_2Cr_2O_7$ and H_2SO_4 then washed with 1:1 HNO_3 followed by a rinsing with the research water. The glassware was cleaned after each set of runs.

The reagents used as supporting electrolytes, KNO_3 and

$(C_2H_5)_4NClO_4$, were Baker and Eastman reagent grades, respectively. The synthesis of ferrocene ($FeCp_2$), the internal standard, required the following reagents: Baker analyzed dimethylsulfoxide, 1,2-dimethoxyethane, hydrochloric acid, and dicyclopentadiene, reagent grade ferrous chloride-4-hydrate from Matheson, Coleman, and Bell, and Fisher reagent grade potassium hydroxide. The preparation of the ylide metallocenes required the sulfonium ylide ($CpSMe_2$) and the phosphonium ylide ($CpPPh_3$) which had previously been prepared by Dr. Norman Holy, the metal halides (MCl_2) were Fisher reagent grade and Baker-Analyzed grade tetrahydrofuran.

C. Preparation of Compounds

The synthesis of bis(cyclopentadienyl)iron(II) (Ferrocene) followed the procedure developed by Jolly.[28]

$$8KOH + 2C_5H_6 + FeCl_2 \cdot 4H_2O \longrightarrow Fe(C_5H_5)_2 + 2KCl + 6KOH \cdot H_2O$$

The cyclopentadiene was first added to a mixture of 1,2-dimethoxyethane and potassium hydroxide. Once these substances dissoved, a solution of iron(II) chloride-4-hydrate in dimethylsulfoxide was slowly added. The resulting solution was added to a slurry of 6 M hydrochloric acid and ice. The precipitated ferrocene was then filtered off. The material was sublimed to obtain a pure sample.

Three of the seven compounds studied were synthesized by others. Dr. Norman Holy prepared $[Ni(CpSMe_2)_2]^{2+}$, Lisa Del Buono prepared the iron ylide metallocene, $[Fe(CpSMe_2)_2]^{2+}$,

and Mo(PC) was obtained from Pfaltz & Bauer, Inc., located in Stamford, Connecticut. A general outline of the procedure used to prepare the ylide metallocenes is shown in Figure 16. By following this procedure, an 85% yield could be obtained.

The tetrahedral iron(II) complex used as a standard to insure that we were performing the redox chemistry on the ylide metallocene was prepared from a method devised by N. S. Gill.[29]

The solvents, acetonitrile and dimethylformamide, which were used to dissolve the ylide metallocenes, were first dried over $MgSO_4$ and then distilled through a "Widmer spiral" fractionating column. Distilling the solvents twice before use produced no significant change on the experimental results.

C. Preparation of Compounds

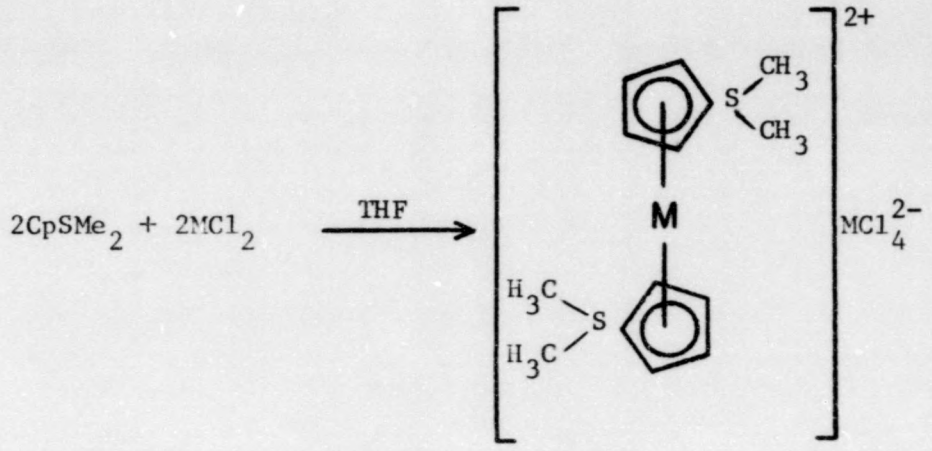

Procedure:

1. A one to one ratio of the ylide and the metal halide is dissolved separately in THF, then simply combined.

2. The precipitated ylide metallocene formed is then filtered quickly.

Figure 16. Procedure for the synthesis of the sulfonium ylide metallocenes.

Note:

The solvent, THF, was first dried over $MgSO_4$ and then distilled. Nitrogen had to be passed continuously over the filtrate because many of the compounds are easily oxidized in air. Once the compound is dried, however, it was relatively stable.

D. Electrodes

1. Hanging Mercury Drop Electrode (HDME)

The first working electrode used in this research was the hanging mercury drop electrode. It was originally

chosen because it appeared to be easier to work with and it was assumed that only the central metal species would be oxidized and/or reduced and therefore would respond to the mercury electrode better. A schematic diagram of the HMDE is shown in Figure 17. After many unsuccessful attempts to obtain cyclic voltammograms of the ylide metallocenes it was concluded that the HMDE was not suitable for this work. It was assumed that the complexes would not respond to the HMDE because of their organic nature.

2. Carbon Paste Electrode (CPE)

The carbon paste electrode is well known for its work with organic compounds.[17] Although this information was initially overlooked, preliminary tests demonstrated the value of this electrode for this research.

A schematic diagram of the CPE is shown in Figure 18. Over the entire anodic potential range, carbon paste electrodes have practically zero residual current, and are therefore far superior to platinum or gold for routine applications. The anodic limits in various media are shown in Table 5. The cathodic limits can be extended to about -1.4V as seen in Table 6. A small, non-removable current appears as a wave at -0.4 to -0.6V. It has been suggested that the wave is due to oxygen dissolved in the carbon paste or absorbed from the test solutions since the size of the peak is decreased upon deaeration. To help combat this current, deaeration time was increased and the electrode left out of the solution until the system was ready to be scanned.

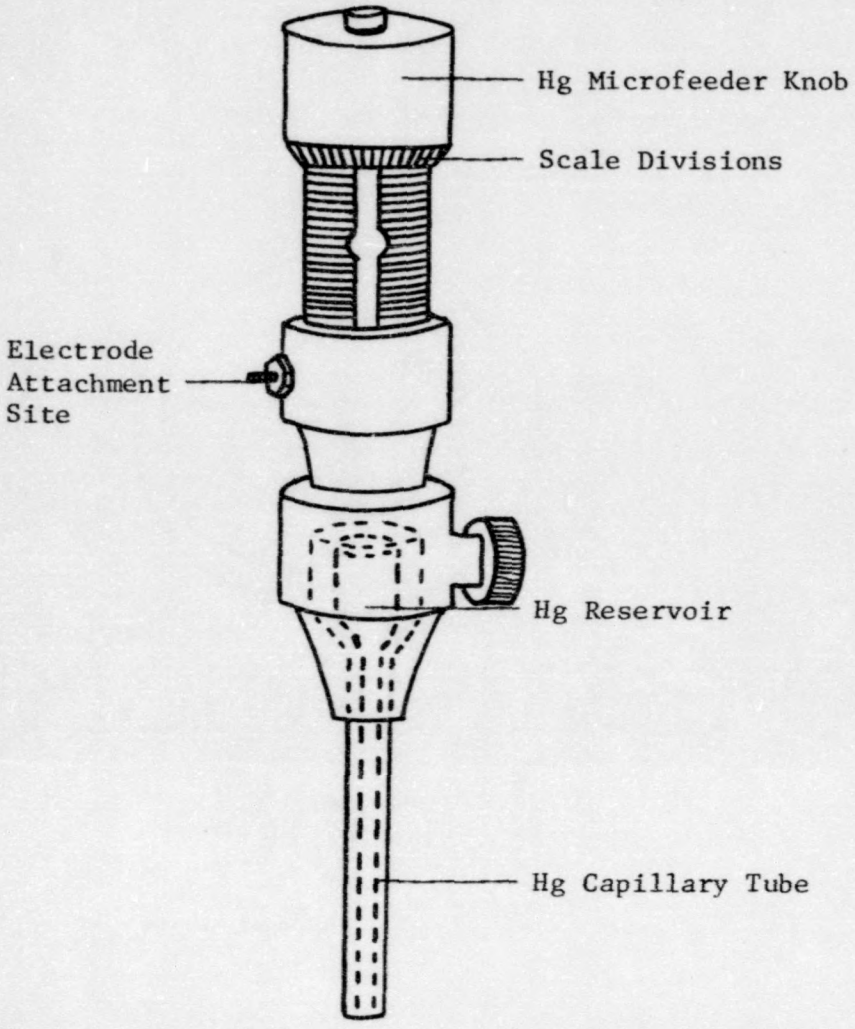

Figure 17. A diagram of the HMDE

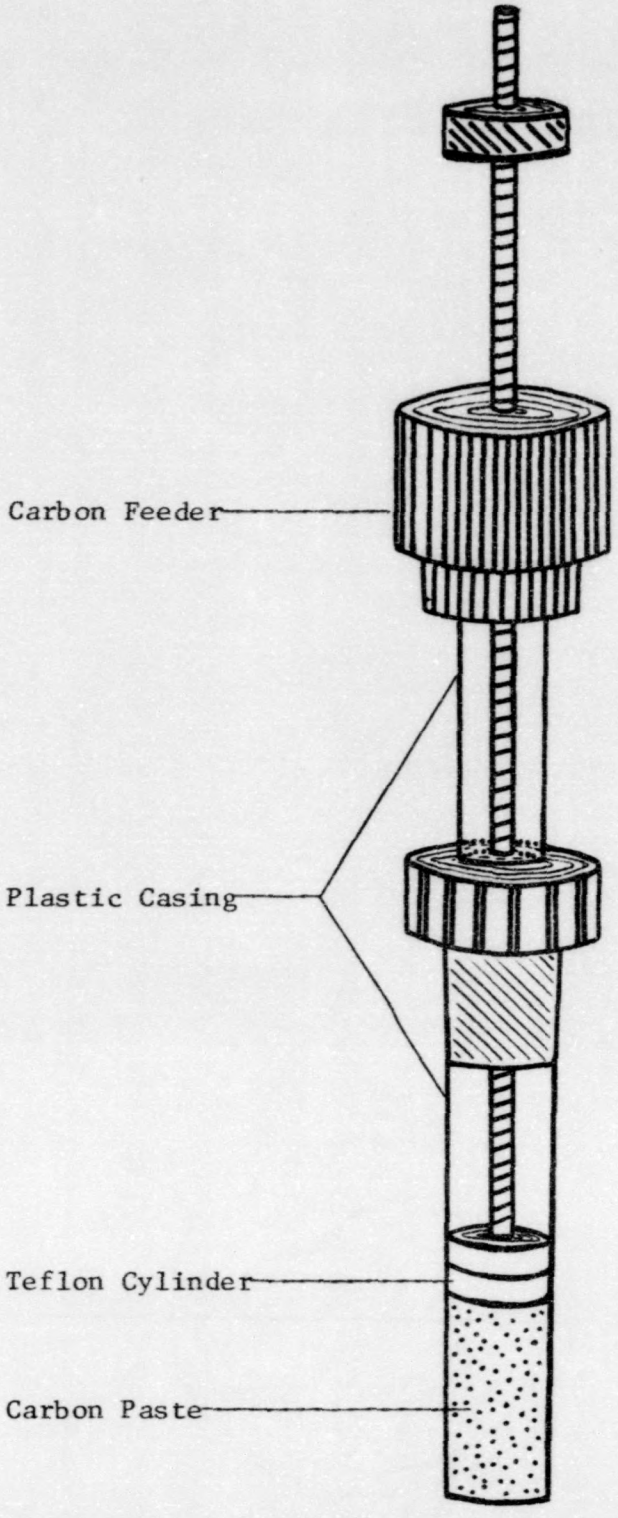

Figure 18. A diagram of the CPE

Table 5

Anodic Limits for Carbon Paste Electrodes

Medium	E vs SCE, V[a]
1M KCl	+1.10
0.1M KCl-HCl, pH 2.5	1.08
1M HCl	1.02
0.1M HAc-NaAc, pH 4.7	1.27
1M Na_2SO_4	1.28
0.1M H_2SO_4	1.30
B and R buffer[b], pH 2.4	1.30
B and R buffer, pH 4.8	1.30
0.2M NaOH	0.87

a - When residual current exceeds 2μA, use carbon electrode-bromonaphthalene paste. When below 2 μA use nujol paste.

b - Britton and Robinson buffer

Table 6

Cathodic Limits for Carbon Paste Electrodes

Medium	E vs SCE, V[a]
1M $HClO_4$	-0.90
1M HCl	-0.90
1M HAc-NaAc	-1.00
1M KNO_3	-1.10
1M KCl	-1.10
1M $NaClO_4$	-1.10
1M NH_3-NH_4Cl	-1.20
1M NaOH	-1.40

a - carbon electrode, nujol paste.

The carbon paste can be prepared by mixing carbon (usually high quality graphite) with a liquid that is sufficiently insoluble in the solvent to prevent the material from dissolving when placed in the test solution. The most frequently used liquids are nujol and bromoform. As seen in Figure 18, the glass tube of the electrode is filled with carbon paste. To obtain the smooth and clean surface required, the following procedure was carried out. A small amount of carbon paste (1/8 in.) was extruded and removed from the electrode. Another small quantity of carbon paste (obtained from the bottled supply that came with the electrode) was placed on an index card. The surface was then smoothed by rubbing the electrode several times across the carbon paste supply. Normally a new surface was prepared for each run when working with organic compounds to circumvent the problem of films that may be deposited during electrolysis. It was found that the weather was a factor in obtaining a smooth and clean surface. During days of high humidity it was much more difficult to obtain a smooth surface than on low humidity days. A new surface could be prepared with practice in approximately 2-5 minutes. Experimental results were reproducible to approximately 5% using the carbon paste electrode.

IV. RESULTS AND DISCUSSION

A. Sulfonium Ylide Metallocenes

1. General Discussion of Ylide Metallocenes

Ferrocene was chosen as the standard for the following reasons: 1) there are references on its redox potentials,[31] 2) it is the most stable metallocene, 3) it can be synthesized easily,[32] and 4) it is the classic metallocene, about which the greatest amount of information is known. The cyclic voltammograms were obtained using a carbon paste electrode (CPE) versus a saturated calomel electrode (SCE).

After obtaining substantial evidence that the system chosen was indeed working and reproducible (by studying ferrocene and comparing the results with the literature), the work with the various transition metal ylide metallocenes specifically chosen by Dr. Norman Holy began. The structural comparison between bis(cyclopentadienyl)iron(II) (ferrocene) and the iron sulfonium ylide metallocene can be seen in Figure 19. The structural differences between the cyclopentadienyl and dimethylsulfonium complexes include alterations in the magnitude and distribution of the charge in the cyclopentadienyl (Cp) ring and also the fact that the ylide complexes are dications. A comparison of the charge distribution between the cyclopentadienyl ring and the sulfonium ylide is shown in Figure 20. Figure 21 shows the various

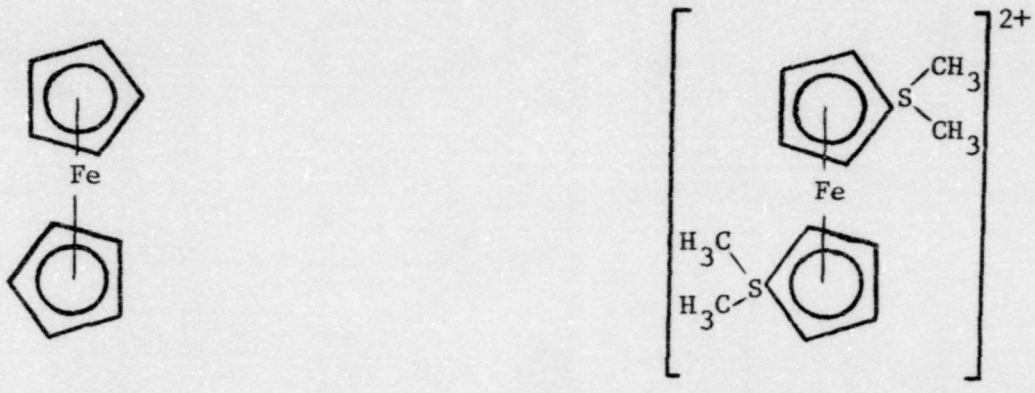

Ferrocene

Iron Sulfonium Ylide Metallocene

Figure 19. A comparison between ferrocene and the iron ylide complex

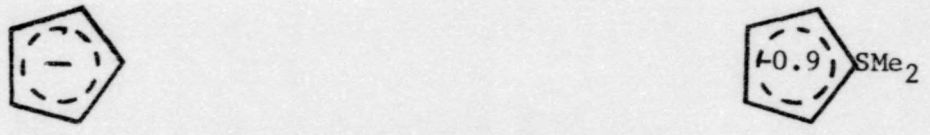

(a) (b)

Figure 20. Distribution of charge of Cp (a) and $CpSMe_2$ (b).[40]

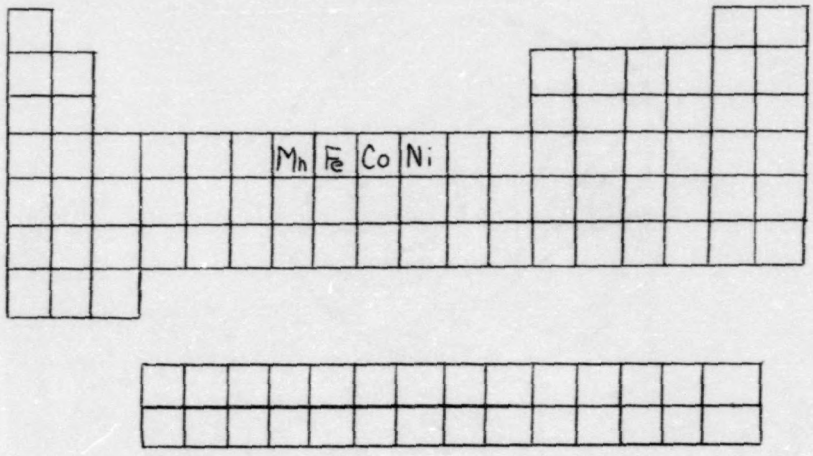

Figure 21. Transition metals that were studied as sulfonium ylide metallocene complexes

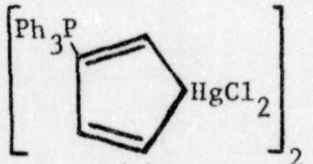

(a)

Mercury(II) Chloride Phosphonium Ylide Complex

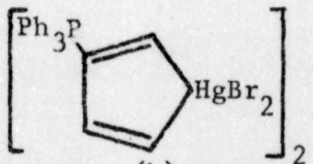

(b)

Mercury(II) Bromide Phosphonium Ylide Complex

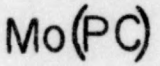

(c)

Molybdenum Phthalocyanine

Figure 22. Remaining compounds that were studied

transition metals that were studied as sulfonium ylide complexes. The remaining compounds that were studied are depicted in Figure 22.

It has been well established that the oxidation or reduction of ferrocene ($FeCp_2$) leads to a one-electron transfer.[33] If ferrocene is reduced, the added electron can be found in one of two places: 1) at the metal atom, or 2) at the cyclopentadienyl rings. Actually, the electron may be in both places, spending an equal amount of time in each.[34] When oxidation occurs, there is a loss of electron density from the metal and the Cp rings. The bulk loss appears to be associated with the metal.

Over the years, the cyclopentadienyl ring system has been studied religiously. A number of workers have predicted the negative charge on the ring to be distributed throughout the entire structure as seen in Figure 23.[35,36]

Figure 23. Predicted negative charge on cyclopentadiene ring

In order to obtain further evidence for this predicted structure, cyclopentadiene-C^{14} was synthesized, having the hydrogen distributed equally throughout the structure.[37] The results are sketched in Figure 24.

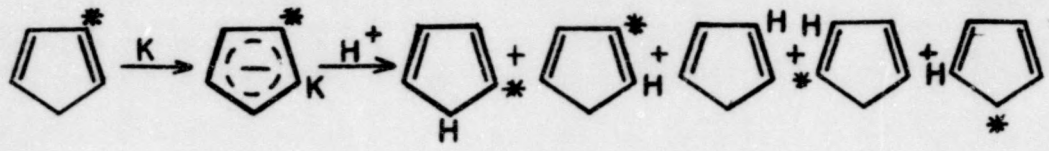

Figure 24. Results of the synthesis of cyclopentadiene-C^{14} having the H equally distributed throughout the structure

Ferrocene has been described as having a staggered (D_{5d}) conformation.[4,5] An approximate molecular orbital (MO) energy-level diagram can be seen in Figure 25. Each cyclopentadienyl ring has five π molecular orbitals, a degenerate antibonding pair (e_2), a degenerate weakly bonding pair (e_1), and one strongly bonding (a) shown in Figure 26.[38] The combined pair of rings has ten π orbitals. If the D_{5d} symmetry is assumed, a center of symmetry exists and there will be antisymmetric (u) combinations and centrosymmetric (g) combinations. This set of orbitals is shown on the left of Figure 25. The valence shell (3d, 4s, 4p) orbitals of the iron atom are shown on the right. A strong interaction exists between the ring π orbitals and the metal's s and p valence orbitals.[39] The overlap of the e_1-type d orbitals (d_{xz} and d_{yz}) of the metal atom with the e_1-type ring π orbitals is the main source of bonding. Figure 27 shows the orbital overlap.

As mentioned previously, ferrocene is the most stable metallocene. The stability comes from containing 18 electrons, an ideal number for metallocene complexes. Each ring donates

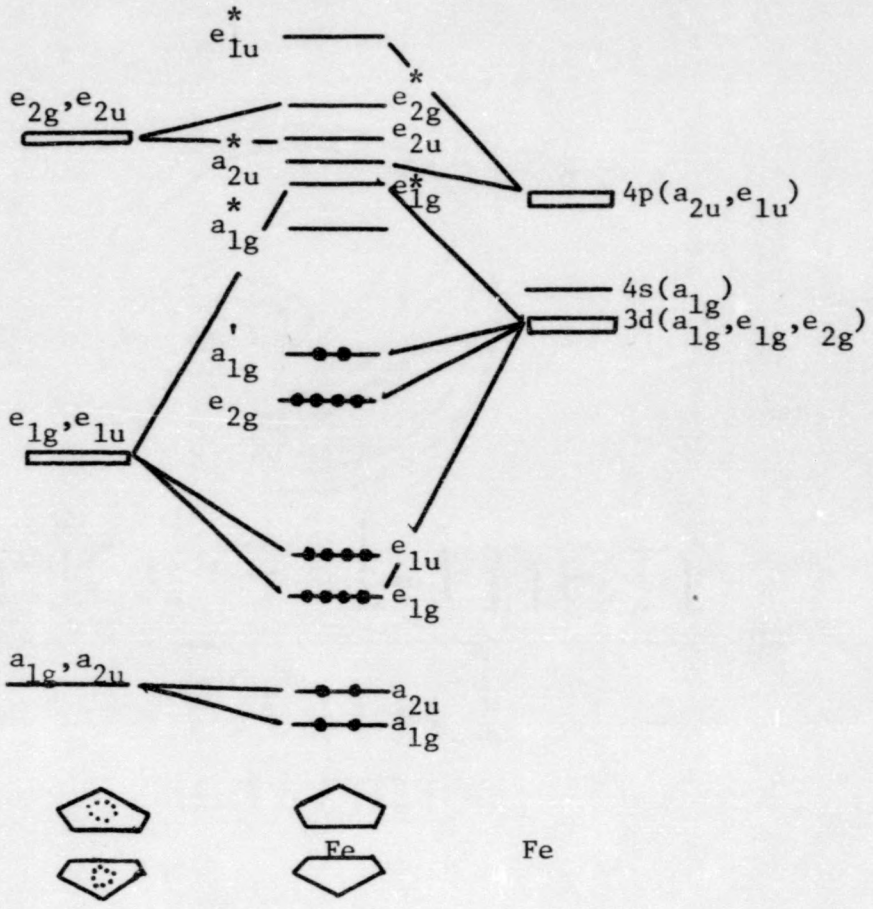

Figure 25. An approximate MO diagram for ferrocene

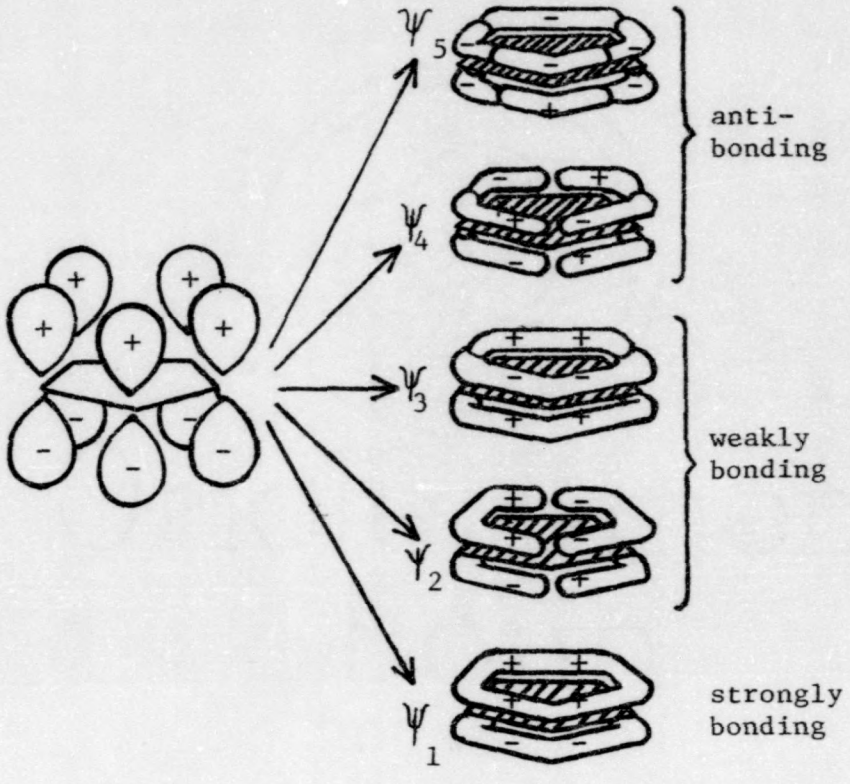

Figure 26. The π molecular orbitals formed from the set of pπ orbitals of the C_5H_5 ring

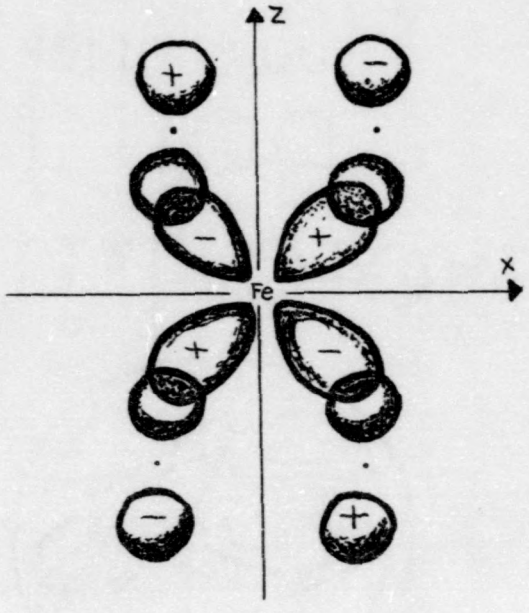

Figure 27. A sketch showing how the d_{xz} orbital overlaps with a ring π orbital to give a delocalized metal-ring bond. The view is a cross-section taken in the xz plane.

six electrons and the iron donates the final six, which fulfills the 18 electron rule by filling the non-bonding e_{2g} and a_{1g} levels. The e_{1u} and e_{1g} ring orbitals contribute very little to the bonding since the 4 p orbitals on the iron are at a high energy state. Only the 3d orbitals are matched well enough to form the two strong pi bonds. The stability of the complex is created by these two bonds.

An ideal applied potential (E) versus current (i) cyclic voltammogram for ferrocene can be seen in Figure 28. Ferrocene has been shown to have a reversible one-electron process. For the $FeCp_2$ system, the difference between the peak potentials (ΔE_p) exceeds the value of $\frac{0.059}{n}$ volts slightly ($\frac{0.059}{n}$ V is a criterion for reversibility). The designation "reversible" is still warranted by the facts that the ΔE_p is still rather small, the peak potentials remain constant when the scan rate is changed, and the ratio of the peak current heights (i_{pa}/i_{pc}) is very close to one. From this data ferrocene was shown to be a reliable standard.

The effect of the dimethylsulfonium group gives added stability to the complexes, thus lower potentials are expected. The sulfur atom is in resonance with the cyclopentadienyl ring seen in Figure 29. This additional delocalization would result in a lowering of the oxidation potentials. The reduction potentials should be lowered as a consequence of the electron withdrawing group (SMe_2) causing the Cp ring to become electron deficient as compared to the cyclopentadienyl ring alone. On the basis of the above points, a trend of lower potentials for the sulfonium ylide complexes was anticipated.

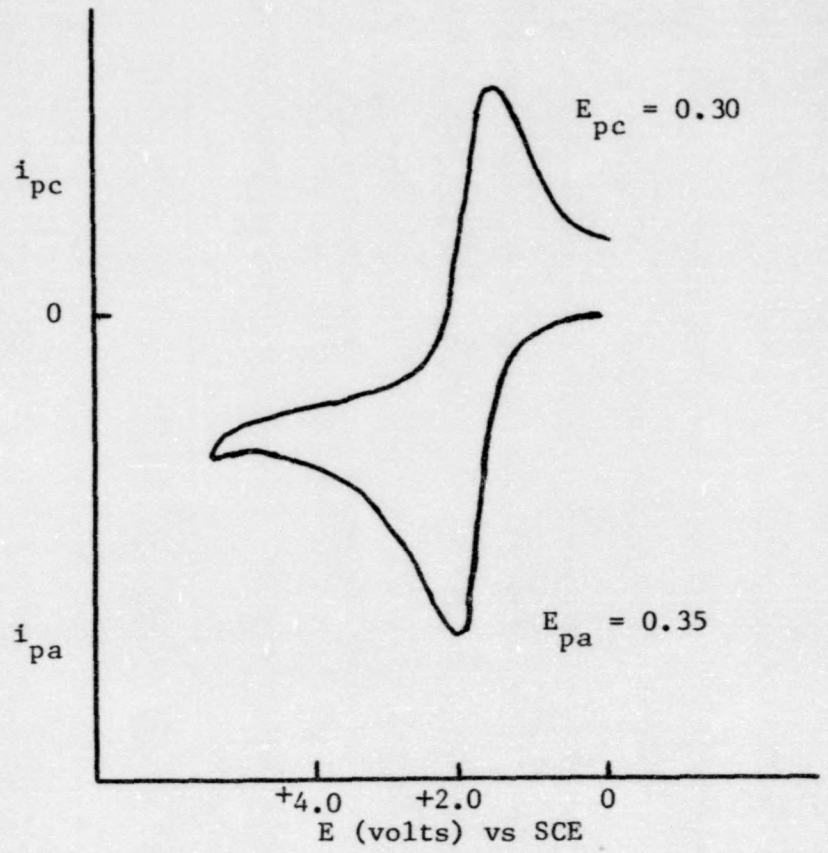

Figure 28. Typical current-voltage curve for ferrocene in an aqueous solution of CH_3CN and 1.0 M KNO_3

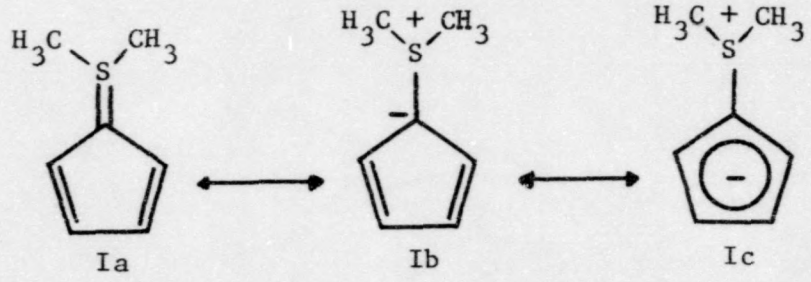

Figure 29. Sulfonium ylide showing resonance.[40]

2. Iron Sulfonium Ylide Metallocene

The iron sulfonium ylide complex $[Fe(CpSMe_2)_2]^{2+}$ is shown in Figure 30. This ylide metallocene was the most stable complex studied. Because of this factor much time and effort was expended to obtain accurate and precise potentials. Before the research on the iron ylide was begun, it was assumed that there would be a good possibility that the electron transfer process would be reversible. This assumption was based on the relative stability of the complex and the fact that ferrocene(which it resembles) is reversible and extremely stable.

The medium used consisted of a mixed solution (15 ml volume) of acetonitrile (10 ml) and 1 M KNO_3 in water (5 ml). The electrolysis cell was purged with nitrogen for five minutes to remove oxygen. This system provided the voltammogram depicted in Figure 31. The appearance of the wave suggests that it may indeed be reversible. The peak current heights (i_{pa} and i_{pc}) look to be approximately equal, and the peak potential separation (ΔE_p) looks as though it may approach the ideal value of $\frac{0.059}{n}$ volts. A further clue of reversibility, the peak potentials remaining constant when the scan rate is changed, was tested. The results are shown in Figure 32. It was concluded that the potentials remained constant.

Another test to prove reversibility consisted of allowing the solution (iron ylide in 10 ml of CH_3CN and 5 ml of 1 M KNO_3 in water) to stand for several minutes (10 minutes)

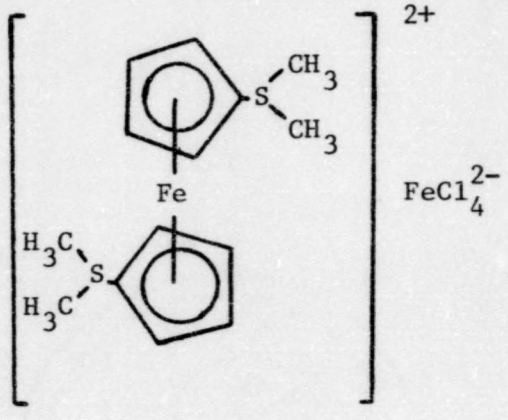

Figure 30. Structure of the iron sulfonium ylide metallocene

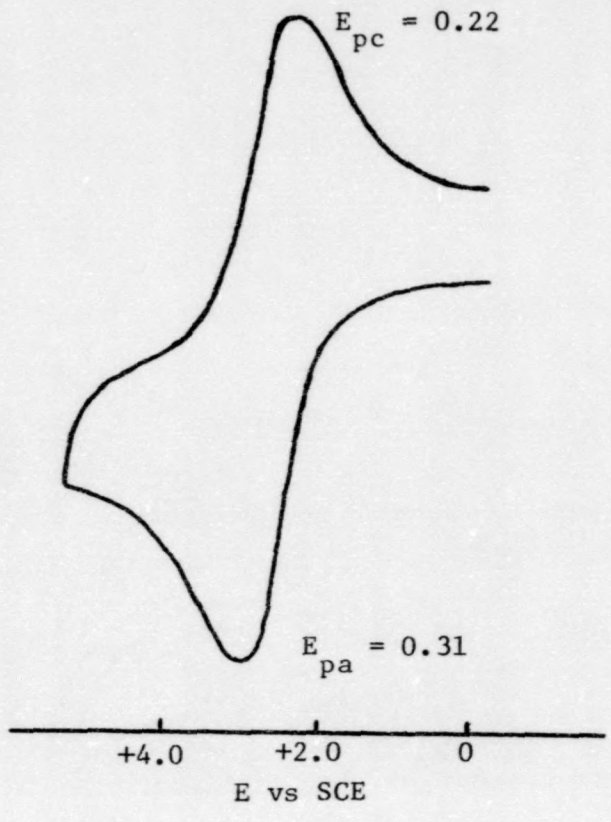

Figure 31. Cyclic voltammogram of $[Fe(CpSMe_2)_2]^{2+}$ using the CPE in 10 ml of acetonitrile and 5 ml of 1 M KNO_3 in water at 23°C

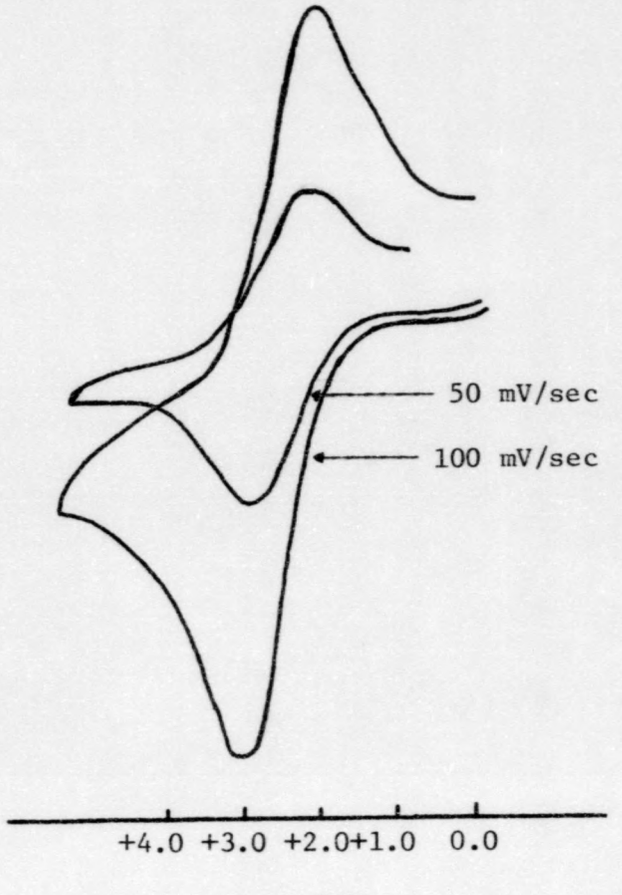

Figure 32. Subsequent scans of $[Fe(CpSMe_2)_2]^{2+}$ at varying scan rates (100 and 50 mV/SEC) showing constant peak potentials (E_p)

after the initial scan, then making a final scan. The wave obtained from this experiment was superimposable on the initial voltammogram.

To summarize the oxidation-reduction process, the following equation would apply,

$$[Fe(II)(CpSMe_2)_2]^{2+} \longrightarrow [Fe(III)(CpSMe_2)_2]^{3+} + e^-$$

indicating there was a one electron reversible transfer process. The conclusion that the redox process is reversible is substantiated by other tests. Plots of the ratio of anodic to cathodic peak current heights versus the square root of the scan rate (Figure 33) and also of anodic or cathodic peak current height versus the square root of the scan rate (Figure 34) are linear, giving further evidence of reversibility. We can also conclude from Figure 14 that the initial species [Fe(II)] is catalytically regenerated after the oxidation step.

3. Manganese Sulfonium Ylide Metallocene

The next ylide metallocene to be discussed is the manganese sulfonium ylide complex, $[Mn(CpSMe_2)_2]^{2+}$. It should be noted that the electrochemical behavior of Manganocene ($MnCp_2$) is not well defined. Manganocene has a tendency to ionize in solvents used for voltammetry, thus making it very difficult to determine its electrochemical behavior.[11] The discussion, therefore, is limited to the behavior of the manganese ylide metallocene.

The manganese sulfonium ylide complex (Figure 35) is quite stable in air. An irreversible voltammogram was

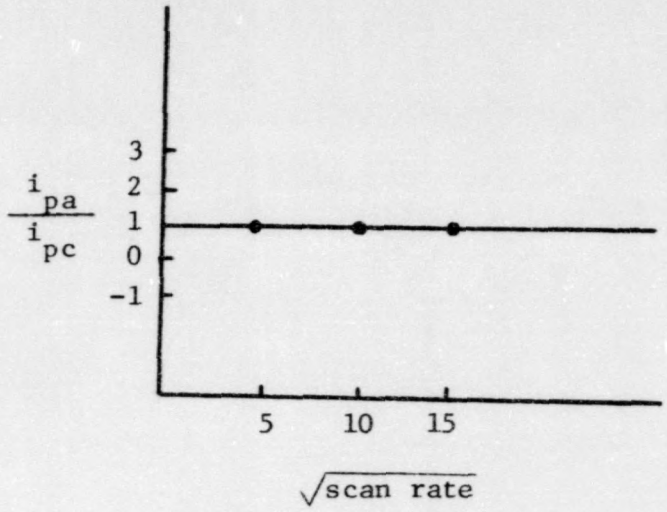

Figure 33. Plot of the ratio of the anodic peak current height (i_{pa}) to cathodic peak current height (i_{pc}) versus the square root of the scan rate showing the reversibility of $[Fe(CpSMe_2)_2]^{2+}$

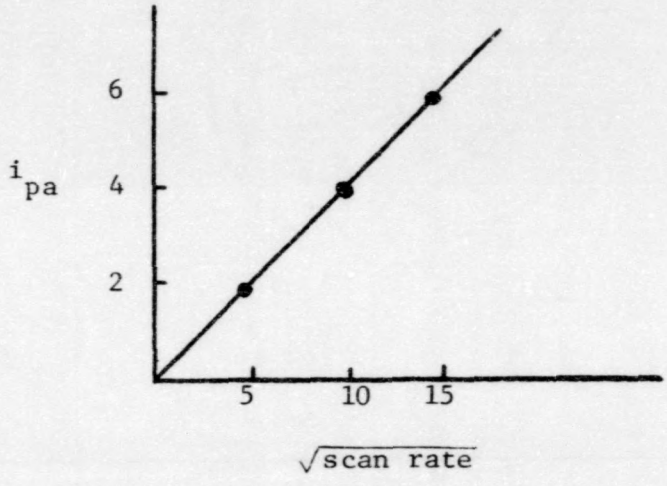

Figure 34. Plot of anodic peak current height (i_{pa}) versus the square root of the scan rate showing linearity and reversibility of $[Fe(CpSMe_2)_2]^{2+}$

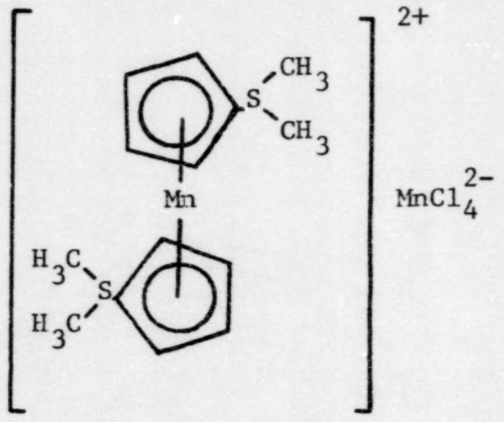

Figure 35. Manganese ylide complex.

obtained with a CPE vs SCE in a mixed solution of 10 ml of acetonitrile and 5 ml of 1 M KNO_3 in water. The cyclic voltammogram is shown in Figure 36. The manganese sulfonium ylide was initially reduced to obtain the Mn(I) complex. The electron transfer process is considered to be irreversible for the following reasons: 1) the difference between the peak potentials (ΔE_p) was greater than $\frac{0.059}{n}$ Volts and 2) there is a large difference between the peak current heights (i_p) of the cathodic and anodic waves. Subsequent scans were made after allowing the solution to stand for several minutes (5, 10 and 15 minutes) which showed that the initial wave was reproducible within approximately 5%. When the scan rate was increased, the positions of the peak potentials remained relatively constant. The ylide solution was a light brown and remained so throughout the entire oxidation-reduction process.

4. Nickel Sulfonium Ylide Metallocene

The nickel ylide metallocene (Figure 37) was the next complex to be studied. This complex was the least stable of all the compounds considered. A possible cause of this instability could be the 20 valence electrons contained in the complex. Because of this instability, special steps had to be taken. Two experiments were performed, each having a separate set of conditions. The first had conditions similar to those performed on the two previous ylide metallocenes. The electrochemical cell was kept at a constant temperature (23°C), and the nickel ylide was placed in a mixed medium of 10 ml of acetonitrile and 5 ml of 1 M KNO_3 in water.

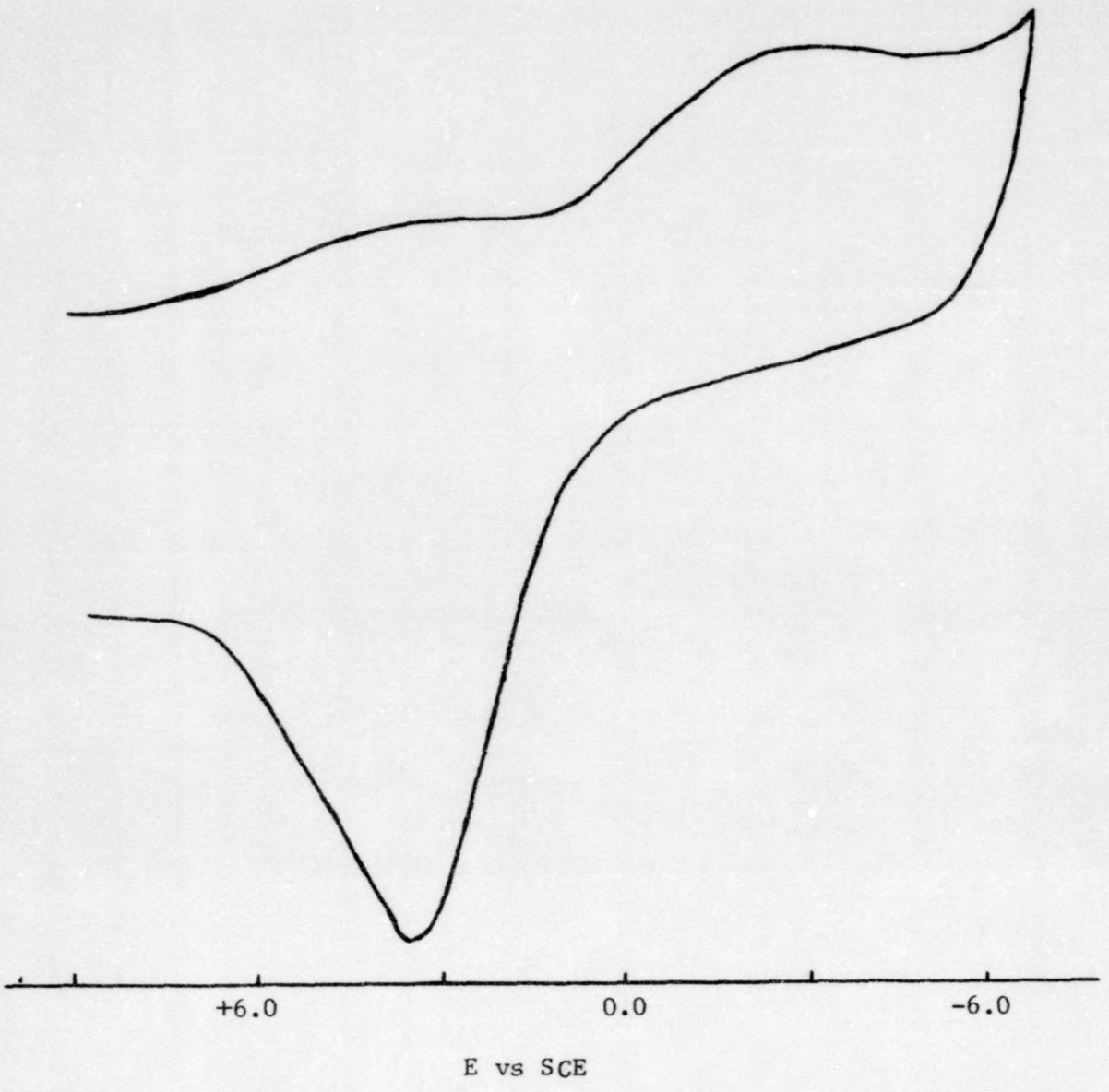

Figure 36. Cyclic voltammogram for $[Mn(CpSMe_2)_2]^{2+}$ in 10 ml of CH_3CN and 5 ml of 1 M KNO_3 in water at 23°C

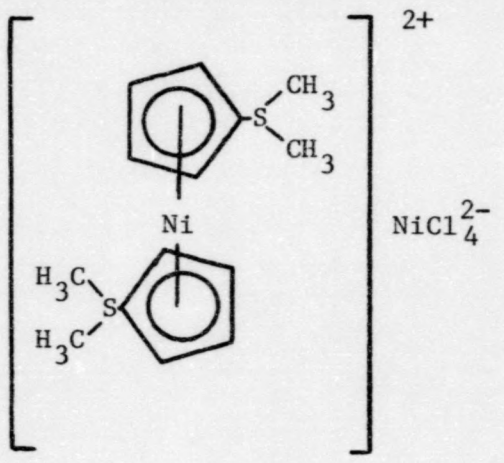

Figure 37. The nickel sulfonium ylide metallocene complex

The one variable that was changed was the length of time nitrogen was passed through the solution. The time was changed from five to sixty minutes in order to insure the removal of oxygen from the solution. The results obtained from this first experiment were not very encouraging. The only substantial wave appeared in the extreme positive end of the scanning window (Figure 38). Looking at the voltammogram, one feature stands out above all others: the cathodic peak potential (E_{pc}) is greater than the anodic peak potential (E_{pa}). This characteristic is opposite from the usual cyclic voltammograms. Although we do not have an explanation for this phenomenon at this time, the nickel ylide appears to be extremely unstable at room temperature which may cause the complex to be changed in some way to give the above voltammogram.

Since the experiment at room temperature gave unsatisfactory results, a second experiment was performed at a lower temperature. A partial vacuum was set up inside the cell at this lower temperature. A schematic diagram of the cell is shown in Figure 39. The temperature inside the cell was lowered to 5°C by pumping water cooled in a mixture of ice, ethyl alcohol, and sodium chloride through the water jacket of the cell. We hoped the use of the partial vacuum and lower temperature would give the complex the added stability needed to obtain reasonable results. The same solvent system was used for the nickel ylide and nitrogen was again passed through the solution for sixty minutes. The voltammogram obtained is shown in Figure 40. The wave appears to be irreversible but subsequent scans indicated it was

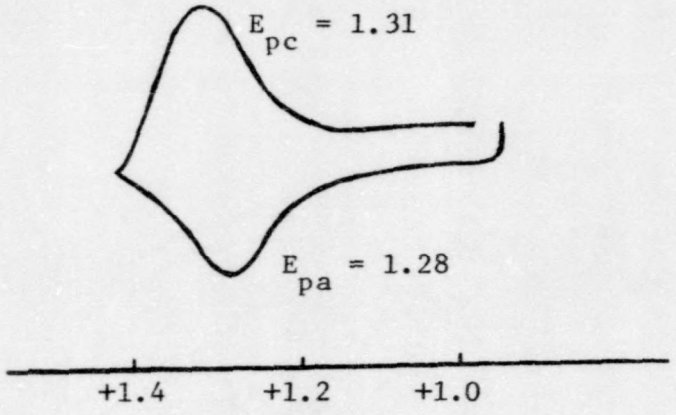

Figure 38. Voltammogram of $[Ni(CpSMe_2)_2]^{2+}$ in 10 ml of CH_3CN and 5 ml of 1 M KNO_3 in water at 23°C

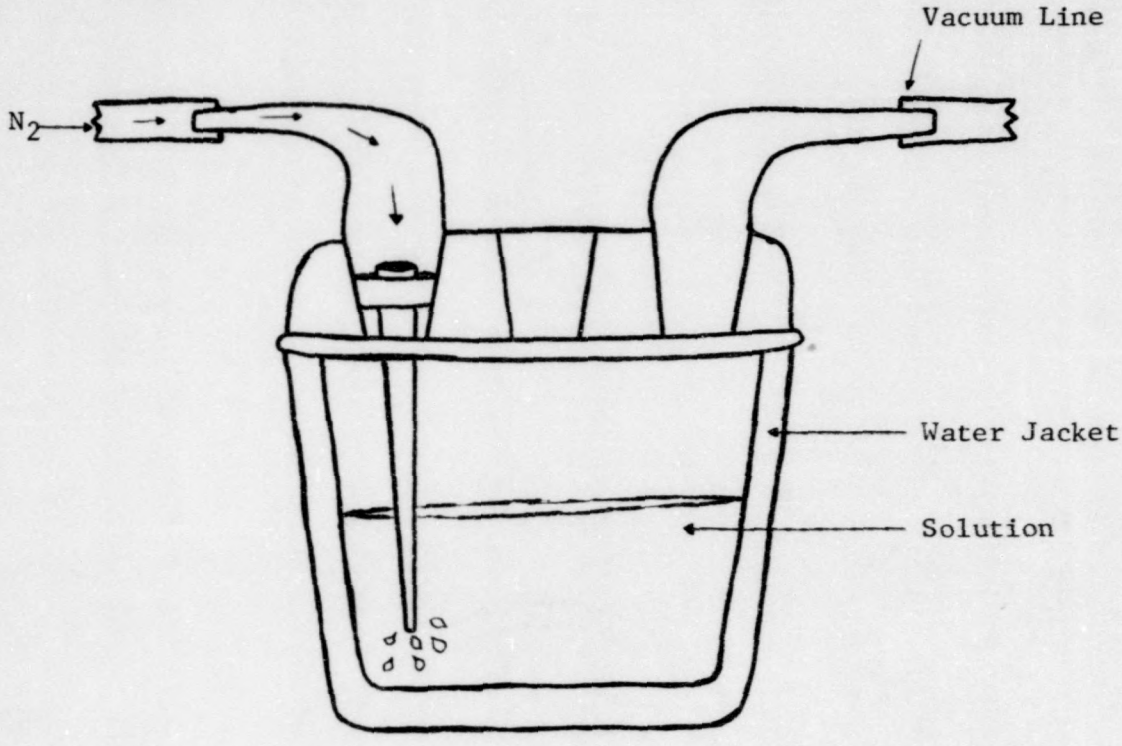

Figure 39. Schematic diagram of the voltammetric cell

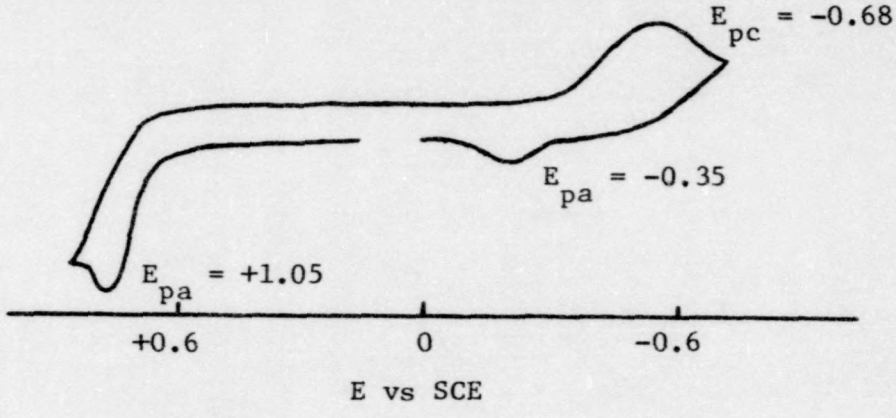

Figure 40. Voltammogram of $[Ni(CpSMe_2)_2]^{2+}$ in 10 ml of CH_3CN and 5 ml of 1 M KNO_3 in water at 5°C

reproducible. The peak at -0.68 volts is probably due to the reduction of Ni(II) to Ni(I). The peak at -0.35 volts gives indication of the Ni(I) species being oxidized to the Ni(II). There is an anodic peak that appears at +1.06 volts which is assumed to be some impurity or possibly the oxidation of Ni(II) to Ni(III). There is not a reduction peak that corresponds to this "possible" oxidation peak. If indeed the peak at +1.06 volts is the oxidation, then the absence of the reduction peak suggests an irreversible electron transfer. As stated previously, this could not be determined.

5. Cobalt Sulfonium Ylide Metallocene

The final sulfonium ylide metallocene to be discussed is the cobalt complex (Figure 41). The medium was changed from a mixed solution of acetonitrile and KNO_3 to a mixed system of acetonitrile (10 ml) and 0.5 M $(C_2H_5)_4NClO_4$ (5 ml) in water because the 1 M KNO_3 seemed to interfere with the electrochemical reactions. Using this new medium and a carbon paste electrode (CPE) the wave shown in Figure 42 was obtained. These observations suggest that the Co(II) species was initially converted to the Co(III). Although the cyclic voltammogram appears to be irreversible, the positions are relatively close together. The voltammogram was shown to be reproducible by making several subsequent scans. There seems to be only one electron transferred in this system represented by

$$Co(CpSMe_2)_2^{3+} + e^- \rightleftharpoons Co(CpSMe_2)_2^{2+}$$

The electron transfer process was shown to be irreversible by the large difference in the peak current heights (i_p).

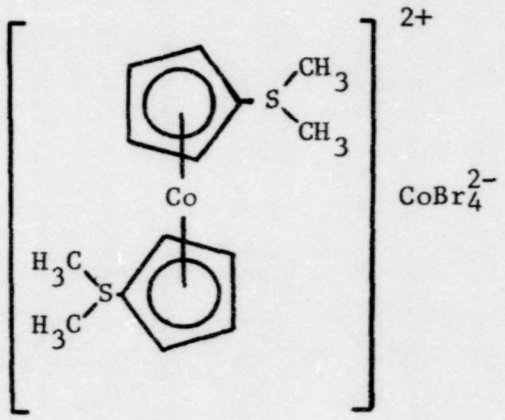

Figure 41. Structure of the cobalt sulfonium ylide metallocene complex

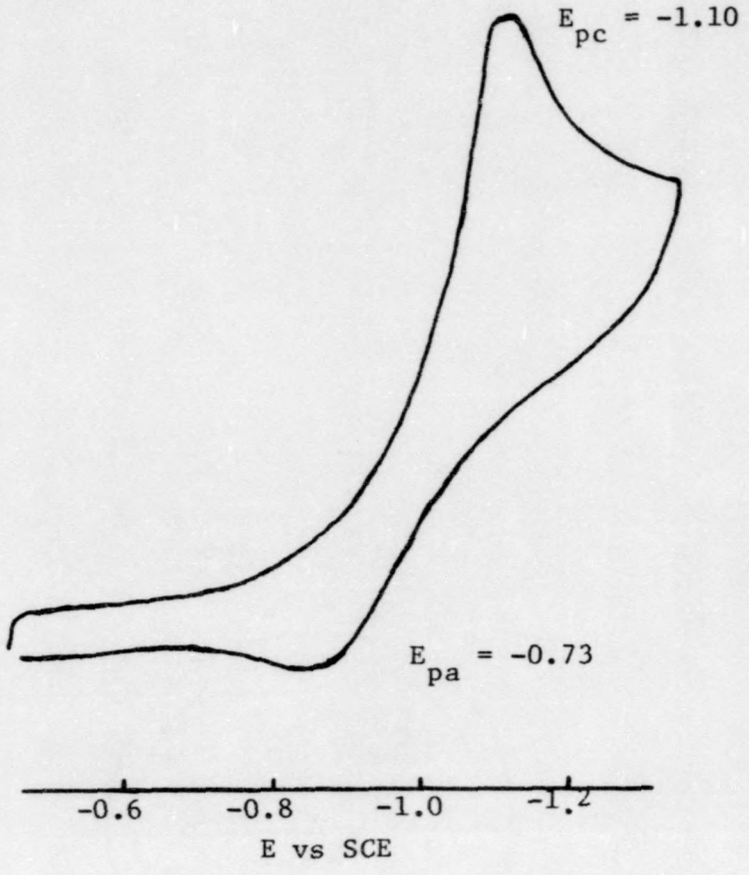

Figure 42. Cyclic voltammogram of $[Co(CpSMe_2)_2]^{2+}$ with a CPE vs SCE, in 10 ml of CH_3CN and 5 ml of 0.5 M $(C_2H_5)_4NClO_4$ in water at 23°C

There is a third (very small) wave at -0.25 volts. This may be some product forming after the oxidation of the Co(II) species. The exact nature of the product is not known at this time. There was not any visible change in the cobalt ylide solution throughout the experimentation. The ylide solution remained light green. Nitrogen was passed through the solution for five minutes to prevent oxygen interference with the cobalt complex.

B. Other Complexes

At this point, all the metallocenes that have been discussed are π complexes. Other types of metallocene complexes have been prepared and were studied in this work. The first to be discussed is the phosphonium ylide mercury bromide complex. This complex was found to be insoluble in acetonitrile, tetrahydrofuran, and other solvents. Finally, the coordinating solvent dimethylformamide (DMF) was used. A nonaqueous, 15 ml solution of DMF containing 0.5 M $(C_2H_5)_4NClO_4$ was used as the medium. Nitrogen was passed through the solution for 10 minutes to remove any oxygen. The cyclic voltammogram obtained from this system was rather complex and is shown in Figure 43. Because the wave was so complicated, no attempt was made to explain it. Instead, the chloride form of the same complex was synthesized with hopes that it would be soluble in a less coordinating solvent since some of the complications are believed to stem from using DMF as the solvent.

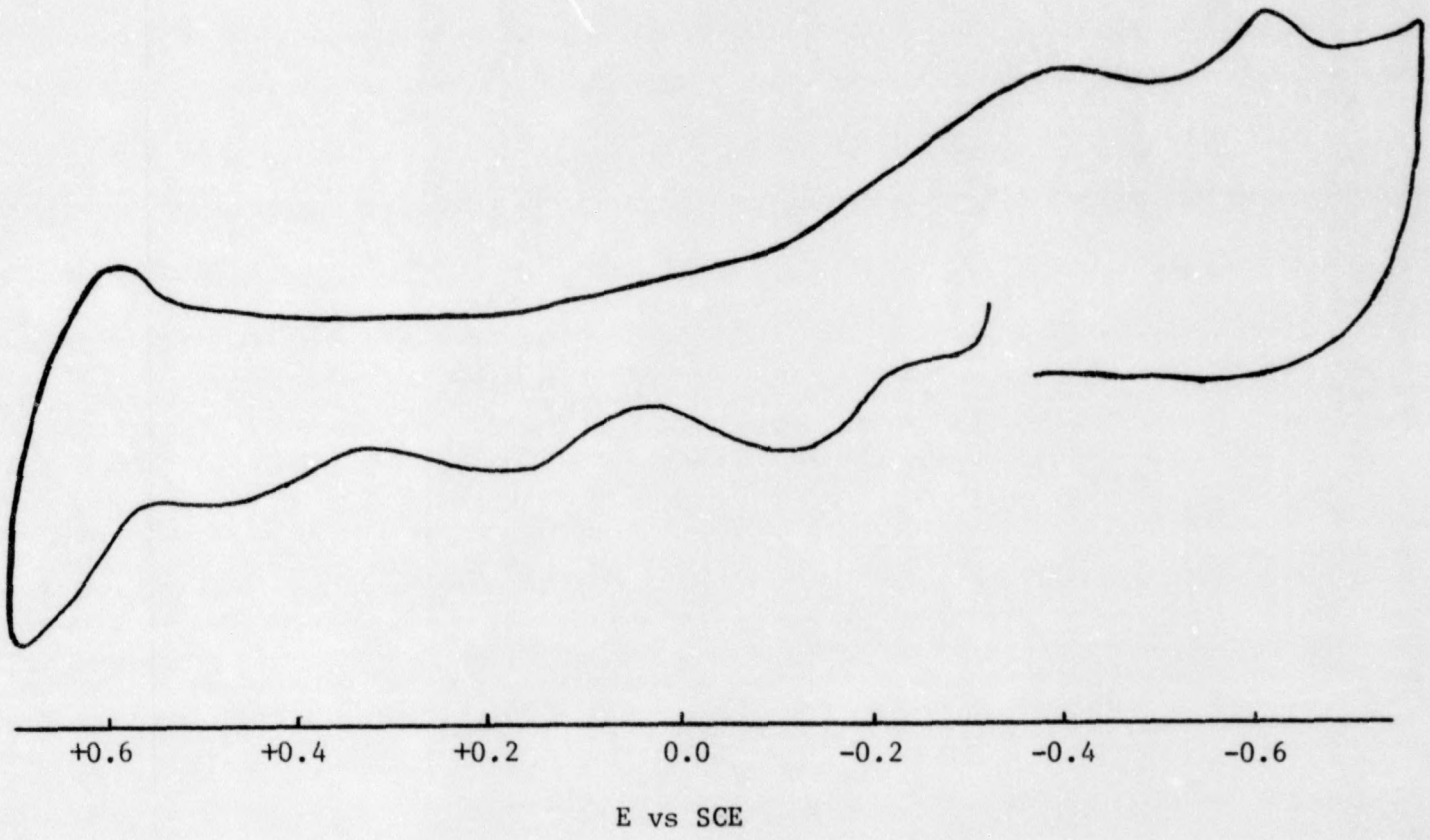

Figure 43. Cyclic voltammogram of $[PPh_3CpHgBr_2]$ with a CPE in DMF containing 0.5 M $(C_2H_5)_4NClO_4$ at 23°C

The phosphonium ylide mercury chloride complex (Figure 22a) was soluble in acetonitrile. A nonaqueous medium of 0.5 M $(C_2H_5)_5NClO_4$ in acetonitrile was used to obtain the wave shown in Figure 44. The voltammogram was reproducible and the peak potentials remained constant when the scan rate was changed. It can only be concluded that the chloride complex under the specified conditions gave the peak potentials depicted in Figure 44.

The final compound studied was molybdenum phthalocyanine [Mo(PC)] (Figure 45). The goal was to obtain some idea of the number of electrons which might be added or removed from the complex. Mo(PC) was soluble in acetonitrile so a non-aqueous solution of 0.5 M $(C_2H_5)_4NClO_4$ in CH_3CN was used. Using a carbon paste electrode the voltammogram in Figure 46 was obtained. Several peaks were expected because it is known that phthalocyanine undergoes several redox reactions. The only substantial peaks that appeared were those shown in Figure 46.

C. Elimination of Interferences

Blank runs of all compounds studied were carefully performed to insure there would be no possible interferences with the actual redox experiments. As mentioned in the previous discussion, two media were used: 1) mixed solutions of acetonitrile (10 ml) and 1 M KNO_3 (5 ml) in water, and 2) nonaqueous solutions of 0.5 M $(C_2H_5)_4NClO_4$ in acetonitrile. These two media did not interfere with the electrochemical reactions of the ylide metallocenes.

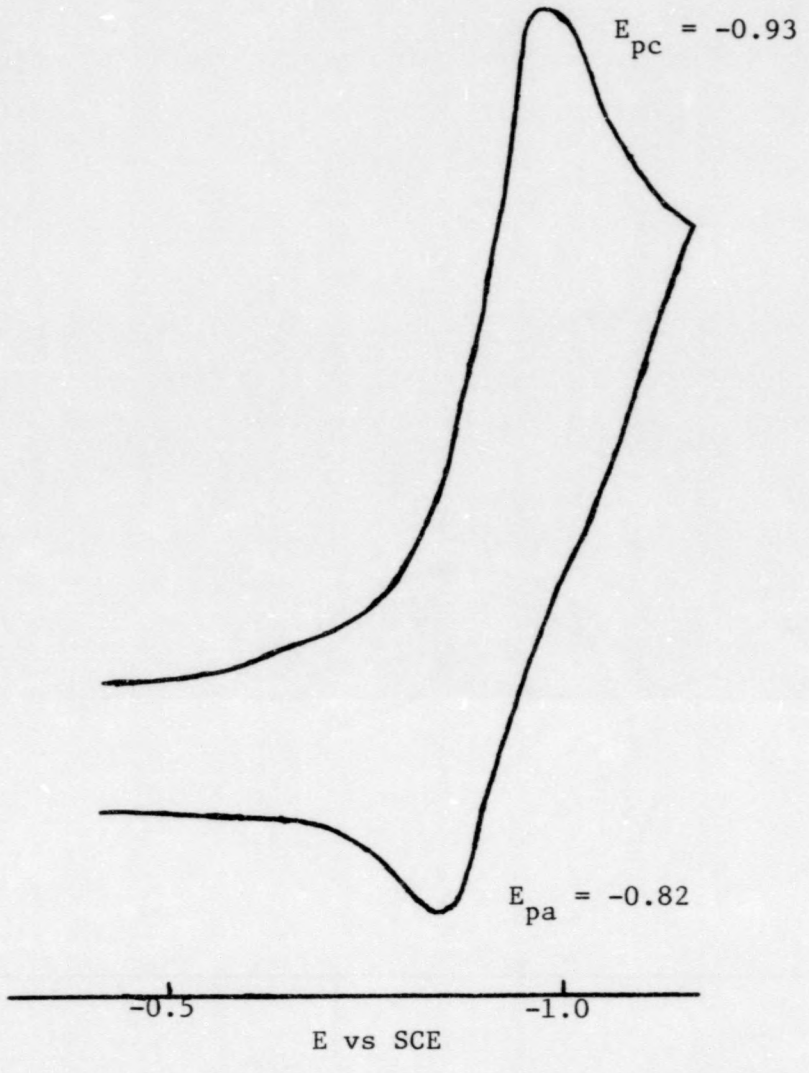

Figure 44. Cyclic voltammogram of $[PPh_3CpHgCl_2]$ with a CPE in CH_3CN containing 0.5 M $(C_2H_5)_4NClO_4$ at 23°C.

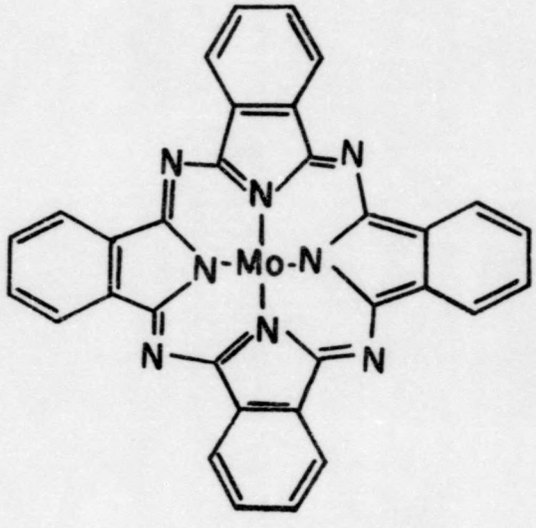

Figure 45. Structure of Mo(PC)

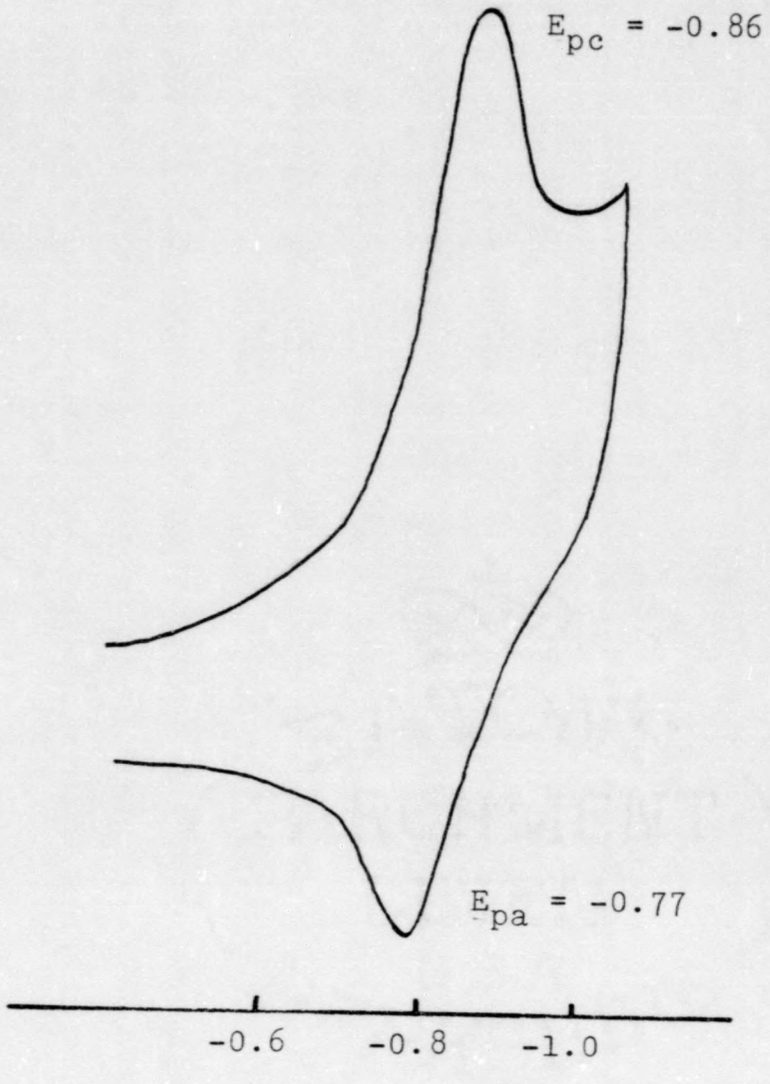

Figure 46. Cyclic voltammogram of Mo(PC) with a CPE in CH_3CN containing 0.5 M $(C_2H_5)_4NClO_4$ at 23°C

Several steps were taken to insure that the complexes being oxidized and/or reduced were the actual ylide metallocenes. Looking at the general structure of the sulfonium ylide metallocene, a tetrahalide salt is complexed to the ylide metallocene (Figure 47). Before concluding the study of the iron sulfonium ylide metallocene, the iron tetrachloride salt was synthesized and a cyclic voltammogram obtained to determine if the tetrachloride salt was oxidized and/or reduced. Only very minor peaks were observed, which were not in the vicinity of the peaks observed for the ylide metallocene. From this we concluded there was no interference from the tetrachloride salts. For other ylide metallocenes cyclic voltammograms were obtained with the XCl_2 salts (where X = Co, Mn). Again, none of the redox potentials of the salts were in the area in which the ylide metallocene's potential appeared. In fact, the potentials were far from the general vicinity of those obtained from the ylide metallocenes.

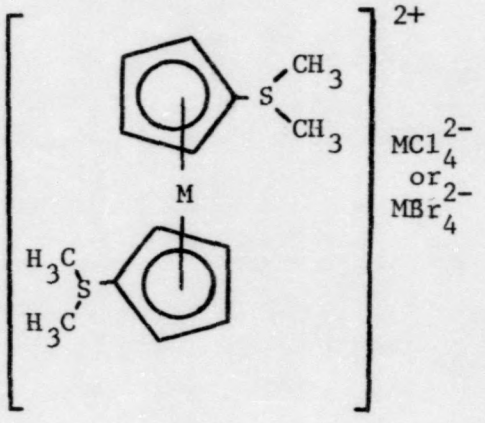

Figure 47. General structure for the sulfonium ylide metallocenes

V. SUMMARY

Now that all the results have been presented, a summary of what has been accomplished can be offered. Figure 48 shows the oxidation and reduction processes for the various ylide metallocene compounds and the ferrocene standard. The ylide metallocenes and ferrocene are shown with their corresponding peak potentials and type of electron transfer. All of the values shown in Figure 48 were obtained from the voltammograms shown previously. It should be noted that the reactions labeled oxidation are those where the scan was begun in the anodic (positive) direction causing oxidation, and those labeled reduction were begun in the cathodic (negative) direction causing reduction.

Recalling from the previous discussion on the reversibility or irreversibility of an electron transfer process, one of the most important criteria was $E_p = \frac{0.059}{n}$ volts, where n is the number of electrons transferred. Table 7 lists the change in the peak potentials (ΔE_p) and the scan rate used for most of the compounds studied. The only compound not shown is the mercury bromide phosphonium ylide complex because it was much too complicated to evaluate. Looking at the iron complex, the ΔE_p is very close to the theoretical value of 0.059 volts. This is the first numerical evidence that suggests it is a reversible system.

Oxidation Processes	E_{pa}(volts)	E_{pc}(volts)	Comments
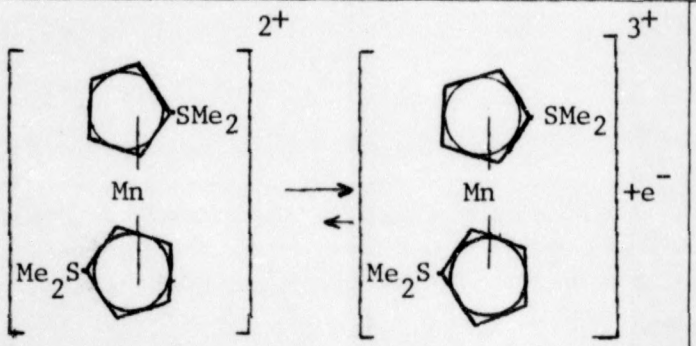	--	--	Mn(II) ⟶ Mn(III) + e^- "irreversible"
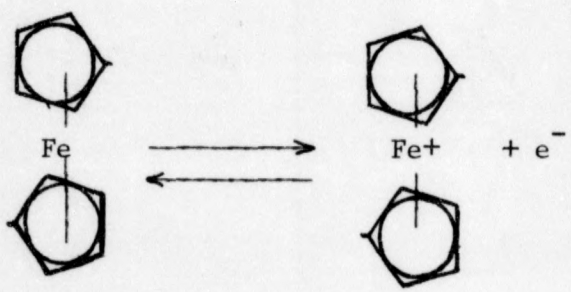	0.35	0.23	Fe(II) ⟶ Fe(III) + e^- "reversible"
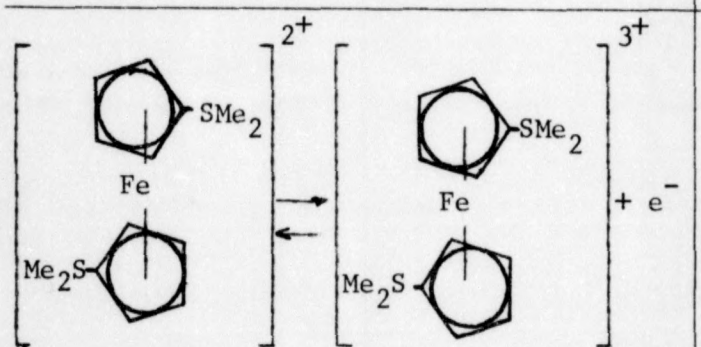	0.31	0.22	Fe(II) ⟶ Fe(III) + e^- "reversible"

Figure 48. Redox Processes for the Ylide Metallocenes
(Figure continued on next page)

Reduction Processes	E_{pa}(volts)	E_{pc}(volts)	Comments
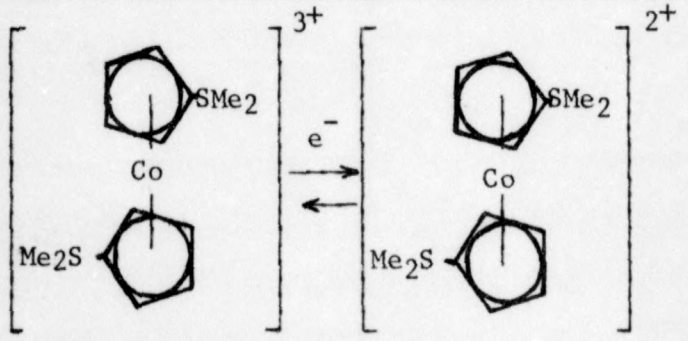	-0.13	-1.10	$Co(III) + e^- \longrightarrow Co(II)$ "irreversible"
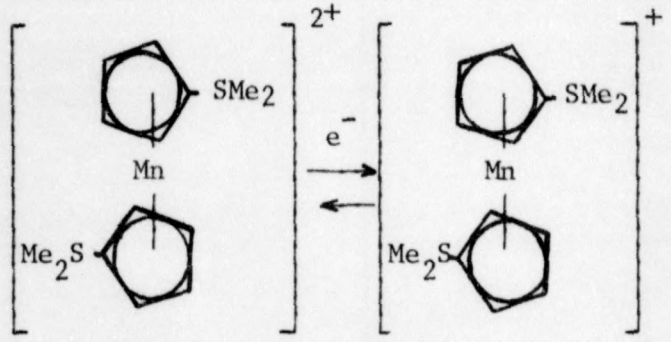	0.41	-0.15	$Mn(II) + e^- \longrightarrow Mn(I)$
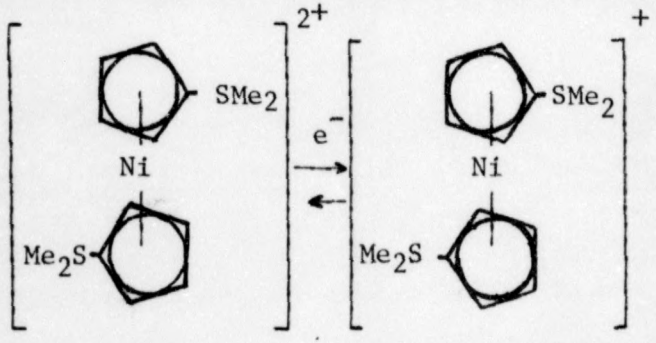	--	-0.67	$Ni(II) + e^- \longrightarrow Ni(I)$ "irreversible"

Figure 48. (Continued from previous page)
Redox Processes for the Ylide Metallocenes

Table 7

Peak Potential Separations (ΔE_p) of

Various Complexes

Compound	ΔE_p (volts)	Scan Rate (mVolts/sec)
$[Mn(CpSMe_2)_2]^{2+}MnCl_4^{2-}$	0.56	200
$FeCp_2$	0.13	200
$[Fe(CpSME_2)_2]^{2+}FeCl_4^{2-}$	0.08	200
$[Co(CpSMe_2)_2]^{3+}CoBr_4^{3-}$	0.37	50
$[Ni(CpSME_2)_2]^{2+}NiCl_4^{2-}$		100
$(Ph_3P)CpHgCl_2$	0.11	100
Mo(PC)	0.09	75

Another important parameter that aids in determining whether or not the electron process is reversible is the ratio of the peak current heights (i_{pa}/i_{pc}). A truly reversible electron transfer would have a ration of 1:1.[10] Table 8 lists the peak current heights (i_p), the ratios, the scan rate, and concentration. The concentration is listed because the peak current height is a function of the concentration. Although this concentration relationship does exist, each wave (anodic and cathodic) is affected equally. Note that for $[Fe(CpSMe_2)_2]^{2+}$ as the scan rate was changed from 0.05 V/sec to 0.200 V/sec the ratio of the peak current heights remained approximately one, a characteristic consistent with reversibility. Table 9 and Figures 49-51 give further evidence to support the assumption that this is a reversible process. Table 9 contains the data used to plot the graphs in Figures 49-51. This information leads us to believe that the iron ylide complex has a reversible one-electron oxidation-reduction process.

The relationship of the half wave potential ($E_{1/2}$) to the peak potential (E_p) (recalling the equation $E_{1/2} = E_p \pm 0.0285$[12]) has been applied to the potentials obtained in this research. The results are tabulated in Table 10. Although this relationship does not depend on the reversibility of a reaction, a reversible electron transfer process would have a more dependable and more accurate ($E_{1/2}$) value since there are fewer constants and coefficients in the related equations.[13]

As stated earlier, some trend in the potentials of the ylide metallocenes versus the potentials of the classical

Table 8

Peak Current Heights and Ratios of the Various Complexes

Compounds	i_{pa} (μAmp)	i_{pc} (μAmp)	i_{pa}/i_{pc}	V(volts/sec)	Concn. mg/15 ml
$[Mn(CpSMe_2)_2]^{2+}$	1.30	4.15	0.25	0.200	3.3
$FeCp_2$	5.10	5.50	0.93	0.100	3.3
$[Fe(CpSMe_2)_2]^{2+}$	8.25 6.00 2.60	8.30 6.10 2.60	0.99 0.98 1.00	0.200 0.100 0.050	3.3
$[Co(CpSMe_2)_2]^{3+}$	0.45	7.9	0.06	0.050	3.3
$[Ni(CpSMe_2)_2]^{2+}$		1.1		0.200	5
$(Ph_3P)CpHgCl_2$	1.9	9.1	0.21	0.100	10
Mo(PC)	1.78	4.23	0.42	0.075	3.3

Table 9

Peak Current Heights with Corresponding Scan Rates for the Iron Ylide Complex

Compound	i_{pa}(μAmp)	i_{pc}(μAmp)	V(volts/S)	$V^{\frac{1}{2}}$
$[Fe(CpSMe_2)_2]^{2+}$	8.25	8.30	0.200	0.447
	6.00	6.10	0.100	0.316
	2.60	2.60	0.050	0.224

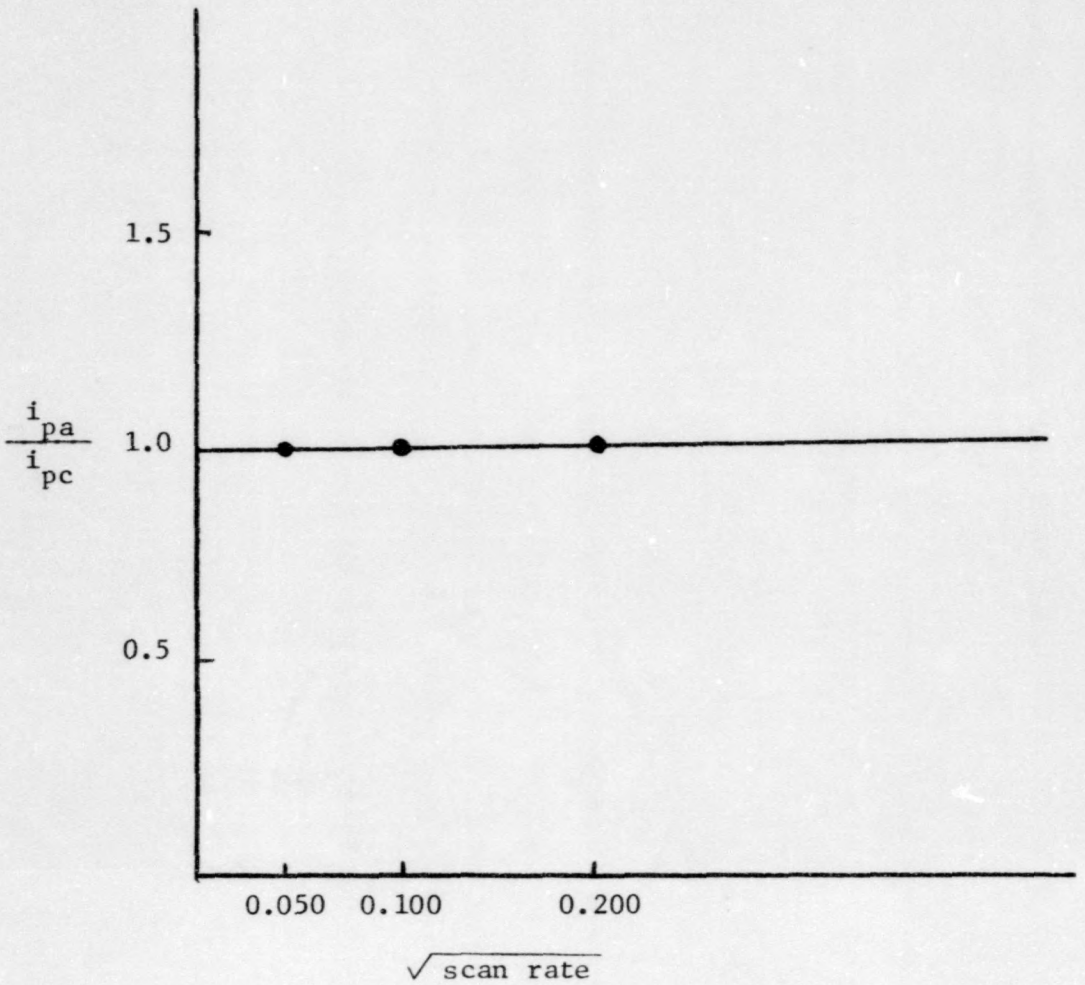

Figure 49. Plot of the ratio of the peak current heights (i_p) versus the square root of the scan rate showing reversibility of $[Fe(CpSMe_2)_2]^{2+}$

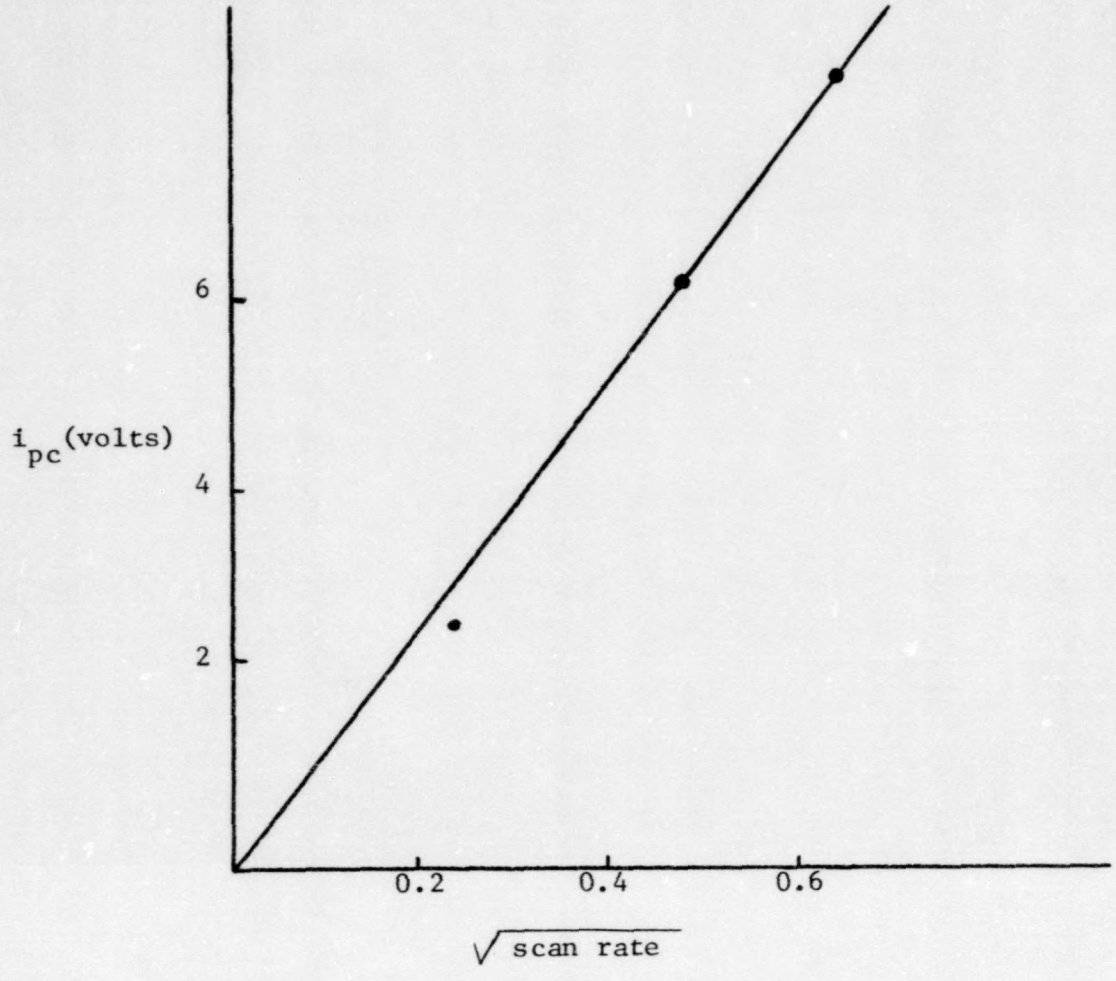

Figure 50. Plot of the cathodic peak current height (i_p) versus the square root of the scan rate showing linearity and reversibility of $[Fe(CpSMe_2)_2]^{2+}$

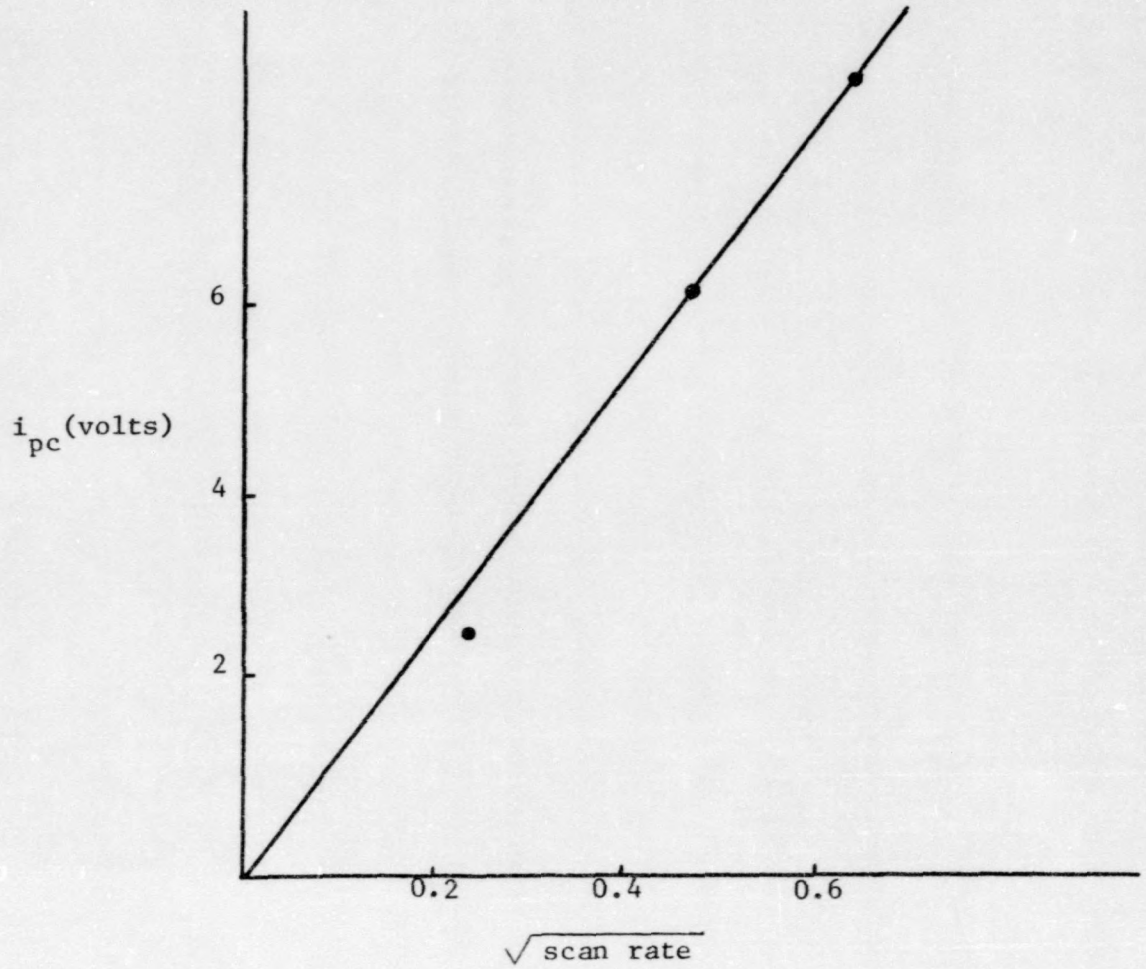

Figure 51. Plot of the anodic peak current height (i_p) versus the square root of the scan rate showing linearity and reversibility of $[Fe(CpSMe_2)_2]^{2+}$

Table 10

Observed

Oxidation-Reduction Potentials of the Various Complexes

Compound	Observed Oxidation Potential ($E^{1/2}$)	Observed Reduction Potential ($E^{1/2}$)
$[Mn(CpSMe_2)_2]^{2+}$	0.38 V	-0.12 V
$FeCp_2$	0.33 V	0.26 V
$[Fe(CpSMe_2)_2]^{2+}$	0.28 V	0.25 V
$[Co(CpSMe_2)_2]^{3+}$	-0.76 V	-1.07 V
$[Ni(CpSMe_2)_2]^{2+}$		-0.70 V
$(Ph_3P)CpHgCl_2$	-0.85 V	-0.99 V
Mo(PC)	-0.79 V	-0.83 V

All values are calculated from: $E_{1/2} = E_{pc} + 0.0285$, $E_{1/2} = E_{pa} - 0.0285$

metallocenes was anticipated. Upon comparing the redox potentials the trend becomes apparent. It was also assumed that the potentials of the ylide metallocenes would be lower than their comparable metallocenes. Table 11 give such a comparison. In looking at the iron ylide complex and comparing it to ferrocene($FeCp_2$), it can be seen that the ylide has an observed half wave potential (oxidation) of 0.28 Volts. Ferrocene has a half-wave potential of 0.33 Volts (literature value of 0.34 volts). Therefore, a difference of approximately 0.05 volts was observed.

Considering the half reactions shown in Figure 48, the Nernst Equation can be written for the iron ylide metallocene

$$E_{1/2}(ox) = E^{o} - 0.059 \log \frac{[Fe(CpSMe_2)_2]^{3+}}{[Fe(CpSMe_2)_2]^{2+}}$$

The lower potentials obtained for the iron ylide complex indicate a decrease in concentration of the Fe(II) species. This suggests that the dimethylsulfonium (SMe_2) group enhances the stability of the complex ($[Fe(CpSMe_2)_2]^{2+}$) as compared to its complimentary pure metallocene $FeCp_2$.

A difference of 0.16 volts was observed between the cathodic peak potentials of the cobalt ylide metallocene (-1.10 volts) and the cobaltocene cation (-0.94 volts). The cathodic peak potential difference between the nickel ylide complex and nickelocene ($NiCp_2$) is 0.58 volts according to the observed values of -0.670 and -0.09 respectively. So, as was anticipated, the trend toward lower potentials for the transition metal ylide metallocenes versus the classical metallocenes was observed.

Table 11

Potentials of the Ylide Complexes versus their Metallocenes

Ylide Metallocene	$E_{1/2}(ox)$	E_{pa}	E_{pc}	ref.	Metallocene	$E_{1/2}(ox)$	E_{pa}	E_{pc}	ref.
$[Fe(CpSMe_2)_2]^{2+}$	0.28	0.31	0.22	this work	$FeCp_2$	0.34	--	--	4
					$FeCp_2$	0.33	0.35	0.23	this work
$[Co(CpSMe_2)_2]^{3+}$	--	-0.73	-1.10	this work	$CoCp_2^+$	--	--	-0.94	5
					$CoCp_2$	--	--	-1.88	5
$[Ni(CpSMe_2)_2]^{2+}$	--	--	-0.67	this work	$NiCp_2$	--	--	-0.09	7

BIBLIOGRAPHY

1. T. J. Kealy and P. L. Pauson, Nature, 168, 1039 (1951).

2. S. A. Miller, J. A. Tebboth, and J. F. Tremaine, J. Chem. Soc., 632 (1952).

3. G. Wilkinson, M. Rosenblum, M. C. Whiting, and R. B. Woodward, J. Am. Chem. Soc., 74, 2125 (1952).

4. P. F. Eiland and R. Pepinsky, J. Am. Chem. Soc., 74, 4971 (1952).

5. J. D. Danitz and L. E. Orgel, Nature, 171, 121 (1953).

6. G. Wilkinson, P. L. Pauson, and F. A. Cotton, J. Am. Chem. Soc., 76, 1970 (1953).

7. R. J. Wilson, L. F. Warren, and M. F. Hawthorne, J. Am. Chem. Soc., 91, 758 (1969).

8. W. E. Geiger, Jr., J. Am. Chem. Soc., 96, 2632 (1974).

9. W. E. Geiger, Jr., J. D. L. Holloway, W. L. Bowden, J. Am. Chem. Soc., 99, 7089 (1977).

10. J. D. L. Holloway, F. C. Senftleber, and W. E. Geiger, Jr., Anal. Chem., 50, 1010 (1978).

11. J. D. L. Holloway and W. E. Geoger, Jr., J. Am. Chem. Soc., 101, 2038 (1979).

12. S. P. Gubin, S. A. Smirnova, and L. I. Denisovich, J. Organomet. Chem., 30, 257 (1971).

13. A. Sevik, Collection Czech. Chem. Commun., 13, 349 (1948).

14. P. T. Kissinger, "Laboratory Techniques in Electroanalytical Chemistry," Dept. of Chem., West Lafayette, IN, Unpublished Manuscript.

15. R. N. Adams, Electrochemistry at Solid Electrodes, New York, N.Y.: Marcel Dekker, Inc., 1969, p. 145.

16. D. Hawley, Ph.D. Thesis, Univ. Kansas, Lawrence, 1965.

17. D. Hawley and R. N. Adams, J. Electroanal. Chem., 10, 376 (1965).

18. W. H. Schwartz and I. Shain, J. Phys. Chem., 70, 845 (1965).

19. R. S. Nicholson, Anal. Chem., 38, 1406 (1960).

20. R. S. Nicholson and I. Shain, Anal. Chem., 36, 706 (1964).

21. R. S. Nicholson, Anal. Chem., 37, 1351 (1965).

22. R. N. Adams, Electrochemistry at Solid Electrodes, New York, N.Y.: Marcel Dekker, Inc., 1969, p. 148.

23. R. Nelson, E. T. Seo, D. Leedy, and R. N. Adams, J. Anal. Chem., 224, 184 (1967).

24. V. D. Parker and L. Eberson, Tetrahedron Lett., 2843 (1969).

25. R. Dietz and B. E. Larcombe, J. Chem. Soc. B, 5, 816 (1970).

26. M. E. Peover and B. S. White, J. Electroanal. Chem., 13, 93 (1967).

27. R. N. Adams, Electrochemistry at Solid Electrodes, New York, N.Y.: Marcel Dekker, Inc., 1969, p. 151.

28. W. L. Jolly, Inorganic Synthesis - Vol. XI, New York, N.Y.: McGraw-Hill Book Co., 1968, p. 120.

29. N. S. Gill, J. Chem. Soc. 3512 (1961).

30. R. N. Adams, Electrochemistry at Solid Electrodes, New York, N.Y.: Marcel Dekker, Inc., 1969, p. 280.

31. M. M. Sabbatini and E. Cessarotti, Inorg. Chem. Acta., 24, L9 (1977).

32. J. A. Page and G. Wilkinson, J. Am. Chem. Soc., 74, 6149 (1952).

33. M. Rosenblum, Chemistry of the Iron Group Metallocenes - Part One, New York, N.Y.: Wiley and Sons, Inc., 1965, p.49.

34. Ibid, p. 51.

35. J. D. Roberts, A. Streitwieser, and C. M. Regan, J. Am. Chem. Soc., 74, 4579 (1952).

36. W. Von D. Doering and J. H. Knox, J. Am. Chem. Soc., 76, 3203 (1954).

37. R. Tkachuk and C. C. Lee, Can. J. Chem., 37, 1644 (1959).

38. F. A. Cotton and G. Wilkinson, Advanced Inorganic Chemistry, New York, N.Y.: John Wiley and Sons, Inc., 1972, p. 741.

39. Ibid, p. 742.

40. Z. Yoshida, S. Yoneda, Y. Murata, J. Organic Chem., 37, 1364 (1972).